ELSEVIER

Contents lists available at ScienceDirect

## Science of the Total Environment

journal homepage: www.elsevier.com/locate/scitotenv





## Dissimilarity of megabenthic community structure between deep-water seamounts with cobalt-rich crusts: Case study in the northwestern Pacific Ocean

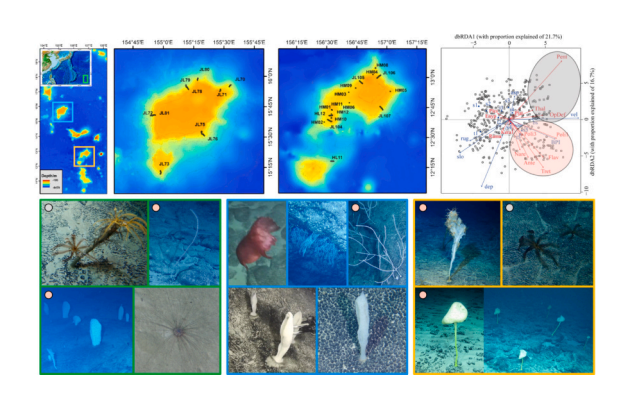
Chengcheng Shen  $^{a,b,c}$ , Runxuan Yan  $^{a,d}$ , Bo Lu  $^{a,c}$ , Zhenggang Li  $^{e}$ , Ruiyan Zhang  $^{a,c}$ , Dongsheng Zhang  $^{a,c,f,*}$ , Chunsheng Wang  $^{a,c,d,f,*}$ 

- a Key Laboratory of Marine Ecosystem Dynamics, Second Institute of Oceanography, Ministry of Natural Resources, Hangzhou 310012, China
- <sup>b</sup> Laoshan Laboratory, Qingdao 266237, China
- <sup>c</sup> Southern Marine Science and Engineering Guangdong Laboratory (Zhuhai), Zhuhai 519000, China
- <sup>d</sup> College of Oceanography, Hohai University, Nanjing 210098, China
- e Key Laboratory of Submarine Geosciences, Second Institute of Oceanography, Ministry of Natural Resources, Hangzhou 310012, China
- <sup>f</sup> School of Oceanography, Shanghai Jiao Tong University, Shanghai 200240, China

## HIGHLIGHTS

- Similar in density, richness, and megafaunal lists between deep-water seamounts
- Dissimilar in the relative abundance of megafauna and assemblage composition
- High patchiness of community structure present throughout seamounts
- Current and microhabitat driving the dissimilarities in community structure

## G R A P H I C A L A B S T R A C T



## ARTICLE INFO

Editor: Olga Pantos

Keywords:
Megafauna
Beta diversity
Vulnerable community
Seamount
Environmental impact
Deep-sea mining

## ABSTRACT

As anthropogenic disturbance on deep-sea seamount ecosystems grows, there is an urgent need for a better understanding of the biodiversity and community structure in benthic ecosystems, which can vary at local and regional scales. A survey of the benthic megafauna on two adjacent deep-water seamounts in the northwestern Pacific Ocean was conducted, which are covered by cobalt-rich crusts, to assess the biodiversity patterns and dissimilarity of assemblage composition. Based on a multidisciplinary dataset generated from video recordings, multibeam bathymetry data, and near-bottom currents, environmental and spatial factors impacting the megabenthic communities were explored. Results showed that these two deep-water seamounts were dominated by hexactinellids, crinoids, and octocorals. The seamounts were able to support diverse and moderately abundant megafauna, with a total of 6436 individuals classified into 94 morphospecies. The survey covered a distance of

E-mail addresses: dszhang@sio.org.cn (D. Zhang), wangsio@sio.org.cn (C. Wang).

https://doi.org/10.1016/j.scitotenv.2024.173914

<sup>\*</sup> Corresponding authors at: Key Laboratory of Marine Ecosystem Dynamics, Second Institute of Oceanography, Ministry of Natural Resources, Hangzhou 310012, China.

52.2 km across a depth range of 1421–3335 m, revealing multiple distinct megabenthic assemblages. The megabenthic communities of the two deep-water seamounts, with comparable environmental conditions, exhibited similarities in overall density, richness, and faunal lists, while dissimilarities in the relative abundance of taxa and assemblage composition. No gradual depth-related change in terms of abundance, richness, or species turnover was observed across the two seamounts, despite the statistical significance of depth in structuring the overall communities. The spatial distribution of megabenthic communities displayed a discontinuous and patchy pattern throughout the two deep-water seamounts. This patchiness was driven by the interactive effects of multiple environmental factors. Near-bottom currents and microhabitat features were the primary drivers influencing their dissimilarities in megabenthic community structure. This case study on the megabenthic community structure of two adjacent seamounts with cobalt-rich crusts can serve as an environmental baseline, providing a reference status for the conservation and management of seamount ecosystems, particularly valuable for areas being considered for deep-sea mining.

#### 1. Introduction

Seamounts are topographically complex features that rise at least 1000 m above the surrounding seafloor and occur throughout the oceans (Rogers, 1994; Yesson et al., 2011). Seamounts provide hard substrates in the deep sea that is dominated by soft-sediment substrates (Bridges et al., 2022), often host diverse and productive benthic fauna, and are proposed to be hotspots of biodiversity in the deep sea (e.g., Victorero et al., 2018). However, threats to seamounts have increased, including overfishing, destructive fishing, marine litter, direct and indirect impacts of climate change, and potentially deep-sea mining activities (Rogers, 2018). Among them, the deep-sea fisheries trawling has been relatively well documented to affect dominant sessile seamount megafauna, and accordingly the concept of vulnerable marine ecosystems as well as their vulnerable indicators (UNGA, 2006; FAO, 2009) has been proposed to assist in the management of deep-sea fisheries (Clark and Koslow, 2007; Goode et al., 2020; Williams et al., 2010). Meanwhile, potential harmful impact of mining activities on deep-sea ecosystems is attracting increasing attention. It was estimated that the cobalt-rich crusts occur on the surfaces of seamounts from their summit margin to steep flanks lower than 3000 m (He et al., 2011). The direct removal of ferromanganese crusts and increased sediment loads are the main disturbances caused by mining activities (Rogers, 2018). They have fatal impact on the filtering or habitat-forming taxa which are often dominant on the seamounts. Knowledge of the biodiversity and community structure within areas targeted for deep-sea mining is crucial for the effective environmental management on mining activities and the sustainability of deep-sea ecosystems.

Since seamounts span a broad range of depths, whether there is a bathymetric gradient of biodiversity on seamounts in the deep sea has attracted significant research interest. The results of diversity-depth relationships can be mixed, varying among taxa and seamounts (see Bridges et al., 2022 for a review). There were case studies documenting depth as a major driver defining clear faunal zonation in the structure of benthic assemblages (Clark et al., 2010; McClain and Lundsten, 2015; Preez et al., 2016), while other research has also illustrated a lack of significant correlation between depth and diversity (Bridges et al., 2022; McClain et al., 2010; Morgan et al., 2015). Nevertheless, significant species turnover with depth has been increasingly recognized (Bridges et al., 2022; Shen et al., 2021; Victorero et al., 2018). Indeed, the presence of different water masses at varying depth has been recognized as a significant factor in shaping the vertical pattern of biodiversity and structure of deep-sea benthic communities (Puerta et al., 2022; Roberts et al., 2021; Victorero et al., 2018). The water masses, with distinctive physical and biogeochemical properties, can indicate more realistic environmental gradients that incorporate depth-related changes in factors like pressure, temperature, salinity, dissolved oxygen, and food availability. Among different seamounts, the depth of summit has been identified as a useful surrogate variable, as varying summit depths will likely mean different levels of overall biodiversity on seamounts (Clark et al., 2011). Seamounts can be classified as shallow, intermediate, or deep-water based on the depth of their summits relative to ecological

zones in the water column (Clark et al., 2011; Yesson et al., 2011). Specifically, seamounts with summits located within the euphotic zone are considered shallow, those with summits within the deep scattering layer (a layer of vertically migrating animals) are considered intermediate, and those with summits below the deep scattering layer are classified as deep-water seamounts. The intermediate seamounts can be highly productive and host significant populations of aggregating reefbuilding species or demersal deep-sea fishes (Yesson et al., 2011). These seamounts have been the focus of investigation due to the development of deep-sea fisheries targeting these seamount ecosystems. In contrast, the deep-water seamounts tend to be less well characterized biologically. The prosperity of benthic communities on deep-water seamounts is commonly limited by the scarcity of particulate organic carbon reaching the deep-water layers (Henson et al., 2012). However, deep-sea water seamounts can benefit from the transport of available food resources by the complex currents in the deep sea. As a result, the benthic fauna on different deep-water seamounts can exhibit variable levels of abundance and species richness (e.g. Morgan et al., 2015; Shen et al., 2021). In addition, the environment of deep-water seamounts tends to be less variable in terms of physical or chemical conditions compared to the shallow and intermediate seamounts which span multiple water layers with distinct properties. Thus, the diverse geological settings and oceanographic processes on deep-water seamounts play a more important role in determining the habitat heterogeneity and benthic distribution, compared to the shallower seamount environments. Accordingly, the biological research on deep-water seamounts has underlined the patchy pattern of benthic fauna throughout seamounts, rather than just the bathymetric gradient, and the environmental drivers in shaping this biodiversity pattern (Morgan et al., 2015; Shen et al., 2021).

Several studies have reported the benthic megafauna inhabiting seamounts with ferromanganese crusts located in the Hawaiian archipelago (Grigg et al., 1987; Schlacher et al., 2014), the mid-Pacific seamounts (Wilson et al., 1985), the Necker Ridge connecting the seamounts of these two areas (Morgan et al., 2015), the Weijia seamount in the northwestern Pacific Ocean (Shen et al., 2021), and the Rio Grande Rise (RGR) in the southern Atlantic Ocean (Corrêa et al., 2022; Perez et al., 2022). An earlier case study on the Cross Seamount (with a summit depth of around 400 m) in the Hawaiian Seamount Chain has indicated that the cobalt-rich crust region exhibited lower overall abundance and species richness of megabenthic fauna (Grigg et al., 1987). Nevertheless, a subsequent study in the Hawaiian Seamount Chain (covering a depth range of 113-1985 m) demonstrated that seamounts with cobalt-rich crusts had no significant differences in species richness but different community structure of benthic megafauna compared to areas outside the cobalt-rich zone (Schlacher et al., 2014). Furthermore, case studies on the Necker Ridge (with a depth range of 1400-2000 m) and the RGR (with a depth range of 600-2000 m) both showed the presence of abundant and diverse megafauna and distinct communities (Corrêa et al., 2022; Morgan et al., 2015; Perez et al., 2018). A case study on the Weijia Seamount (with a depth range of 1533-2763 m), a typical guyot in the northwestern Pacific Ocean,

highlighted the highly patchy pattern and distinct communities within a single seamount, while it showed a lower overall abundance of benthic megafauna compared to that in the Necker Ridge within the deep-water layer (Shen et al., 2021). Although population genetic studies have indicated that dispersal distance of deep-sea fauna is generally greater for taxa inhabiting deeper environments (Baco et al., 2016), the specific patterns of similarity and difference in benthic communities among deep-water seamounts require further investigation.

Taking the Caiwei and Weijia Seamounts in the northwestern Pacific Ocean as examples, two deep-water seamounts located within the cobalt-rich ferromanganese crust exploration contract area of the China Ocean Mineral Resources Research & Development (COMRA), this study explored the megabenthic communities of these seamounts and their differences in community structure. By doing so, we hope to increase the scientific understanding of benthic communities and ecosystems on deep-water seamounts to promote their conservation and sustainable development.

## 2. Materials and methods

#### 2.1. Study seamounts

The northwestern Pacific Ocean is characterized by a dense concentration of seamounts and is also an area enriched in cobalt-rich crusts (Hein, 2002). The Caiwei Seamount and Weijia Seamount, known respectively as Pallada and Ita Mai Tai in the General Bathymetric Chart of the Oceans (GEBCO), lie in the Magellan Seamount Chain in the northwestern Pacific Ocean (Fig. 1A–B). The straight-line distance between the centers of two seamounts is approximately 350 km. Each

seamount is a typical guyot, featuring a flat, platform-like top and steep flanks, and can be categorized as deep-water seamounts, with their average summit depths being lower than 1450 m (Fig. 1C-D; Supplementary Table 1). In southwest of each seamount, there is a relatively smaller neighboring seamount, named the Caiqi Seamount (without a GEBCO name) and the Weixie Seamount (with the GEBCO name Gelendzhik), respectively (Fig. 1C–D). These four seamount names were proposed by COMRA and published by COMRA Office (2017). These names are used throughout this study, rather than the GEBCO names, for consistency since a GEBCO name is not available for the Caiqi Seamount. The phrases of Caiwei Seamounts (CWS) and Weijia Seamounts (WJS) also contain the relevant neighboring seamounts for simplicity. To date, several studies have reported new insights on the benthic megafauna of these seamounts, including the identification of several novel species, evidence of effective dispersal capacity of ophiuroids between the two seamounts (Na et al., 2021), a patchy distribution pattern of megabenthic communities in the Weijia Seamount (Shen et al., 2021), and the relationship between the geomorphology and occurrence of benthic megafauna in the Caiwei Seamount (Fan et al., 2022). Thus, a comprehensive synthesis comparing the megabenthic community structures of the two adjacent deep-water seamounts is urgently needed. Such an analysis should utilize quantitative methods and comparable datasets across the two seamounts.

## 2.2. Data collection and processing

## 2.2.1. Video data collection and taxonomic identification

The data for this study were collected by 6 cruises from 2013 to 2020 (Supplementary Table 2). Video materials totaling 130.83 h were

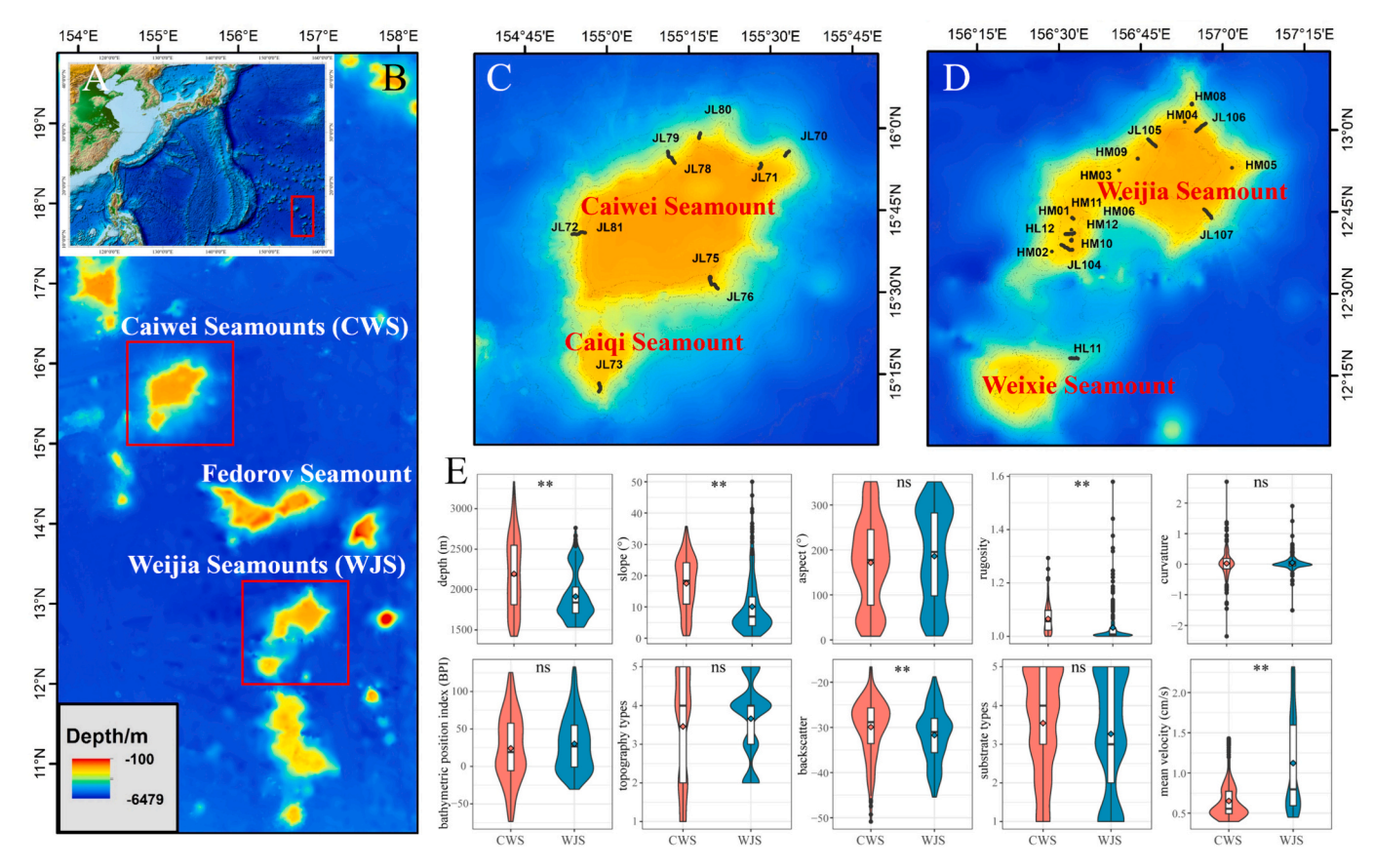


**Fig. 1.** Map of study area in the northwestern Pacific (A) and the relative location of the studied seamounts (B), including the Caiwei and Caiqi Seamounts (C) and the Weijia and Weixie Seamounts (D). Violin and boxplot of each seamount for environmental variables with the Mann-Whitney U test (E). JL = HOV Jiaolong tracks; HM = ROV Haima tracks; HL = ROV Hailong tracks. \*\* = p < 0.01; ns = p > 0.05; the diamond shows the average of environmental variable.

collected during 27 dives using the human occupied vehicle (HOV) Jiaolong, remotely operated vehicle (ROV) Haima, and ROV Hailong III (Fig. 1 C-D; Supplementary Table 2). These dives covered a depth range of 1421-3335 m, and a total distance of 60.3 km near the seabed. The video transects were strategically placed to comprehensively cover each direction of the Caiwei and Weijia Seamounts and at least one transect was positioned on the steep flanks of each of their neighboring seamounts (the Caigi and Weixie Seamounts, respectively). The camera definition and illumination of HOV Jiaolong, ROVs Haima and Hailong III are comparable, as demonstrated in a previous study conducted in the Weijia Seamount (Shen et al., 2021). After discarding poor-quality video segments due to factors such as low light, high altitude above the seabed, fast vehicle speeds, or high level of suspended solids (Shen et al., 2021), the remaining effective video materials covered a total distance of 52.2 km (Supplementary Table 2). These video data were used to identify and count the megabenthic organisms.

The megafauna observed in the videos were identified to the species or morphospecies (organisms that were morphologically distinct) level (Supplementary Table 3), and fishes were counted as a single morphotype, consistent with the approach used in the previous study conducted in the Weijia Seamount (Shen et al., 2021). The taxonomy was updated according to the check-list provided by the World Register of Marine Species (WoRMS: <a href="http://www.marinespecies.org/">http://www.marinespecies.org/</a>), and the taxonomic nomenclature followed the recommendations of Horton et al. (2021). In addition, any megafauna individuals insufficiently clear to identify were classified as unclear fauna and excluded from the statistical analyses. The biological traits for each morphospecies, including movement, living habit, and feeding habit, were designated according to relevant literatures (Rogacheva et al., 2012; Rowden et al., 2016) and direct observations from the video materials (Supplementary Table 4).

## 2.2.2. Substrate and environmental data processing

According to the previous study conducted in the Weijia Seamount (Shen et al., 2021), eight environmental variables were analyzed, including substrate types, depth, slope, aspect, curvature, rugosity, bathymetric position index (BPI), and topographic types. Among them, substrate type was categorized into five classes based on the coverage of sediments observed within constant-distance samples visible in the video materials. The five substrate types were soft, moderately soft, mixed, moderately hard, and hard. The terrain-derived parameters were extracted from shipborne multi-beam bathymetric data with a spatial resolution of 50 m. The parameters of BPI and slope were then used to classify the seabed into five topographic types, including low depression area, moderately depressed area, flat area, moderately elevated area, and highly elevated area.

Furthermore, two additional environmental variables were also used in this study, including backscatter intensity and average velocity of near-bottom currents. The backscatter data, with a resolution of 50 m, were acquired using the ship's hull-mounted Kongsberg EM122 echosounder, concurrently with the bathymetric data, and then processed using the CARIS HIPS and SIPS 9.1 software. The velocity of near-bottom currents was extracted from the hydrodynamic environment of the Northwestern Pacific Ocean, which was simulated using the Coastal and Regional Ocean Community (CROCO) model with a horizontal resolution of  $1/36^{\circ}$ , and the daily average current velocities were calculated for the period from 2011 to 2015, as reported by Jiang et al. (2021).

The position of each transect was determined by combining the ultrashort baseline (USBL) tracking data from the submersible vehicles with the global positioning system (GPS) tracking data from the ship. Each video transect was divided into continuous 100 m samples, as this sample size had been previously demonstrated to effectively characterize the distribution of megafauna in the study area (Shen et al., 2021).

In total, 522 samples were generated to count individual numbers of megafauna and classify the substrate types. To calculate the terrain-related parameters and backscatter intensity at a resolution of 50 m (the same to the resolution of raw bathymetric data), each 100 m sample was further divided into two 50 m segments. The values of these environmental variables for each sample were then assigned as the average of the two corresponding 50 m segment values. The velocity of near-bottom currents was interpolated to match the 100 m sample size using the Kriging method.

### 2.3. Statistical analyses

Statistical analyses were conducted using the open-source R software package, version 4.2.2. Mann-Whitney U test was performed to determine if there were significant differences in each environmental variable between the two seamounts. Kruskal-Wallis test was conducted to investigate significant differences in the environmental variables among the identified clusters as well as differences in the beta diversity. Spearman correlation analysis was performed to assess the association between pairs of environmental variables. To evaluate the sampling efforts, species accumulation curves were plotted for each seamount (Gotelli and Colwell, 2001). Rarefaction curves were plotted for each sample to show the expected number of species as the individual number increasing (Heck et al., 1975). The Locally Weighted Scatterplot Smoothing (Loess) method was used to estimate the underlying trends of abundance and biodiversity along the depth gradient.

Noise clustering was conducted to distinguish the megafaunal assemblages (De Cáceres et al., 2010) and a multidimensional scaling (MDS) ordination plot was then used to visualize the partitioning of the samples (Borcard et al., 2018). This clustering method is considered a more realistic way to describe the similarity among samples (Borcard et al., 2018), since it calculates the weights of samples allocated to each cluster and then discriminates equivocal samples as unclassified, based on their constant distance to the cluster centroid. To examine the spatial variability in the megafaunal community, two methods were used to calculate the beta diversity. One is the total variance based on the Hellinger-transformed species abundance matrix which can be then decomposed to assess the contribution of each species and sample to the overall beta diversity using the beta.div function (Legendre and De Cáceres, 2013). The other is the Jaccard dissimilarity which is then partitioned to assess the relative importance of different ecological processes, including species replacement and richness/abundance differences, affecting the beta diversity using the beta.div.comp function (Legendre, 2014).

To examine the impacts of environmental variables on community distribution, the distance-based redundancy analysis (dbRDA) with forward selection was performed (Blanchet et al., 2008; Legendre and Anderson, 1999), by using a Bray-Curtis dissimilarity matrix after excluding morphospecies occurring only once and empty samples. Also, a dbRDA was performed using the Jaccard dissimilarity matrix, which was further partitioned into matrices representing species replacement and richness/abundance differences, to assess the influences of environmental variables on the overall beta diversity and its underlying ecological processes. Furthermore, the common impacts of environmental and spatial factors were assessed using spatial analyses with a combination of a distance-based Moran's eigenvector map (dbMEM) analysis and variation partitioning (Dray et al., 2006; Legendre and Legendre, 2012). The significant spatial axes from the dbMEM analysis were regressed against the environmental factors (Borcard et al., 2018) to examine the correlations between broad-scale and fine-scale spatial factors and the environmental variables.

The Sørensen index was adopted to quantify the biological similarity between the two seamounts. It is calculated as:

 $Sørensen\ index = 2\times (the\ number\ of\ morphospecies\ observed\ in\ both\ seamounts)/(the\ number\ of\ morphospecies\ observed\ in\ the\ WJS)$   $+\ the\ number\ of\ morphospecies\ observed\ in\ the\ WJS)$ 

When comparing the species composition, the Sørensen index is also called a species richness similarity index. Using the formula provided, the similarity index of assemblages is calculated by considering the assemblage numbers identified in the two seamounts. The distinct assemblages are primarily classified by the clustering method applied in this study.

#### 3. Results

#### 3.1. Environmental conditions

The effective video materials used to make analyses covered a total distance of 52.2 km across the flanks of deep-water seamounts, at depths of 1421-3335 m. The substrate types observed varied, with hard substrates accounting for 31.0 % of the samples (100 m long per sample), while mixed and soft substrates each made up about 20 %. In terms of topography types, 63.0 % of the samples were located in moderately or highly elevated areas, while 12.8 % were situated in flat areas. The boxplot comparisons of environmental variables between the two seamounts are shown in Fig. 1E. Mann-Whitney U test was performed for each environmental variable to investigate the variability between the two seamounts at depths of 1421-3335 m (Fig. 1E). Depth, two terrainrelated variables (slope and rugosity), backscatter, and mean velocity of near-bottom current showed significant (p < 0.01) variability between the two seamounts. Four other terrain-related variables (aspect, curvature, BPI, and topography types) and substrate type showed no statistically significant inter-seamount variability.

Spearman correlation analysis was performed for each pair of environmental variables (Supplementary Fig. 1). Depth was significantly correlated with five terrain-related variables (BPI, topography type, slope, aspect, and rugosity) and substrate type. Substrate type was significantly correlated with all other environmental variables. Current velocity was significantly correlated with three terrain-related variables (slope, rugosity, and curvature), backscatter, and substrate type. BPI was significantly correlated with most other environmental variables, but not with current velocity.

## 3.2. Faunal composition

Total of 6436 megabenthic individuals were counted and classified into 94 morphospecies, with 15 of them observed only once; additionally, 37 unclear sponges, 9 unclear actinians, 6 unclear corals, 4 unclear asteroids, 37 unclear crinoids, 25 unclear holothurians, 1 unclear echinoid, and 59 unclear and unknown individuals were observed. Of the total individuals, 43.8 % were found living on the CWS. The density of megabenthos, calculated based on individuals per 100 m of linear observation, was approximately 12.3 ind./100 m on both the CWS and WJS. Among the total 94 morphospecies identified, 70 were observed on the CWS and 66 on the WJS, with 47 morphospecies common on both seamounts. The accumulation curves of species richness did not reach an asymptote, and the megafaunal diversity on the CWS may potentially be higher than that observed on the WJS (Fig. 2A).

The benthic megafauna in the two seamounts mainly comprised five phyla: Porifera, Cnidaria, Echinodermata, Arthropoda, and Chordata. Echinoderms contributed the highest proportion at 38.1 % of the total individuals, largely composed of crinoids (22.7 %) and ophiuroids (10.4 %); sponges contributed 34.5 % of the total, dominated by hexactinellids (glass sponges); cnidarians contributed 17.7 %, with octoorals being

highly dominant; and fishes made up 4.2 % (Fig. 2B). Sponges dominated the CWS, contributing 43.8 % of the total individuals observed in the CWS, followed by corals at 25.8 %; however, in the WJS, echinoderms dominated and contributed 56.6 %. The total richness similarity index between the two seamounts was calculated at 69.1 %, which increased to 77.7 % when excluding the morphospecies observed only once. The similarity indices were comparable for Porifera (62.9 %) and Echinodermata (65.4 %); the Cnidaria exhibited a relatively higher similarity index (78.0 %), with corals reaching 80.0 % (Fig. 2B).

The biological traits of each morphospecies, including their movement, living habit, and feeding habit, were investigated (Fig. 2C–E). In general, sessile megabenthos occupied for 53.8 % of the individuals, while mobile organisms comprised 35.3 %. In the CWS, sessile taxa dominated at 72.5 %, while in the WJS, mobile taxa occupied for 54.7 %. Considering living habit, taxa that lived independently were the most dominant, occupying for 79.9 % of the total individuals across both seamounts. In terms of feeding habit, suspension feeders were the most prevalent, making up 52.1 %, followed by filter feeders at 34.5 %. The suspension feeders dominated in the WJS (65.1 %), while the filter feeders dominated in the CWS (44.1 %).

Two morphospecies stood out as particularly dominant across the two seamounts (Fig. 2F–G). One was a sponge morphospecies, *Poliopogon* spp. 1 columnar indet., which was more abundant in the CWS but observed more frequently in the WJS; the other was a crinoid morphospecies, Pentametrocrinidae spp. indet., which was largely observed in the WJS. Additionally, two other morphospecies were relatively abundant but less frequently observed, the sponge *Poliopogon* spp. 3 cratered indet. and the coral *Ramuligorgia militaris*, both of which were only found in the CWS. Another sponge morphospecies, *Flavovirens hemiglobus* sp. inc., was observed only in the WJS and was relatively abundant but less frequent in its occurrence. In addition, two unclassified morphotypes, fishes and shrimps, were observed frequently across both seamounts.

## 3.3. Assemblage composition

Noise clustering was performed for morphospecies abundance to investigate the megabenthic community structure on the flanks of the two seamounts at depths of 1421–3335 m. The biotic data of one-occurred morphospecies, unclear taxa, and the two unclassified morphotypes (fishes and shrimps) were excluded. This left a dataset of 72 morphospecies and 420 samples (189 from the CWS and 231 from the WJS) for analysis. Results showed that eight clusters were obviously divided, with an additional 40.0 % of the samples remaining unclassified (Fig. 3A–B). Boxplots depicting the nine environmental variables for each cluster are showed in Fig. 3C.

Among the eight assemblages clustered, one assemblage (Fig. 4, M1, 12.7 % of samples from the CWS) characterized by the preferentially swimming holothurians, *Enypniastes eximia*, was observed on the upper slope of the CWS at depths of 1532–2506 m. The environmental characteristics related to these samples were relatively diverse, largely with mixed to hard substrates located in flat to highly elevated areas, while the mean speed of near-bottom current was relatively lower.

There were three assemblages almost exclusively observed in the WJS. (1) Aggregations of blade-like sponges (*Tretopleura weijica* sp. inc.) with attached unstalked crinoids (Antedonidae spp. indet.) were located on the northeastern slopes (Fig. 4, M2, 5.2 % of WJS samples). (2) Aggregations dominated by stalked sponges (*Flavovirens hemiglobus* sp. inc.) along with the blade-like sponges (*Tretopleura weijica* sp. inc.) were

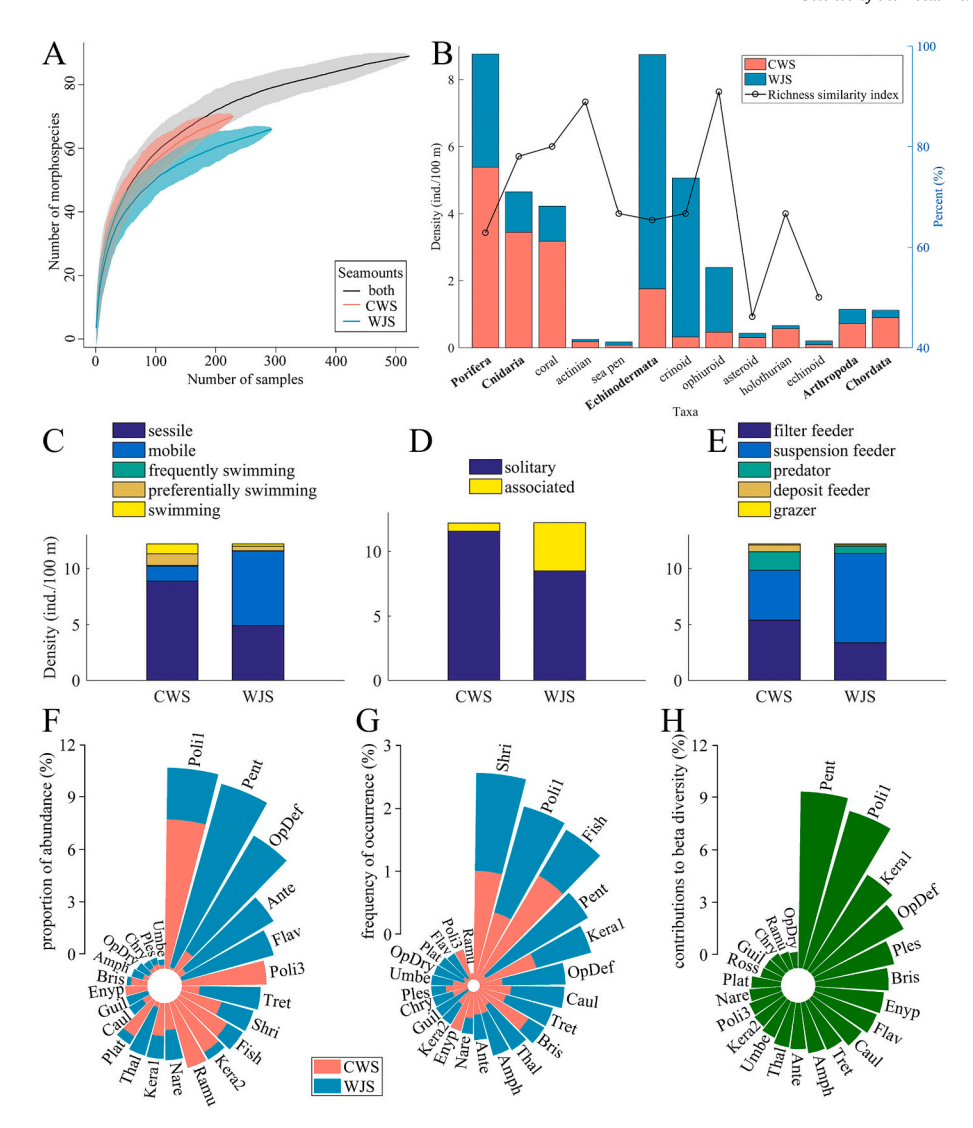


Fig. 2. Accumulation curves of species richness of the Caiwei Seamounts (=CWS), Weijia Seamounts (=WJS) and both (A); density of individuals, by linear observation, for each taxon and the richness similarity index between the CWS and WJS (B); density of individuals relevant to different biological traits including movement (C), living habit (D), and feeding habit (E); the 24 morphospecies including the top 23 of abundance proportion (F) or frequency of occurrence (G) and their contributions to variance-based total beta diversity (H). Hexactinellida: Poli1 (Poliopogon spp. 1 columnar indet.), Flav (Flavovirens hemiglobus sp. inc.), Poli3 (Poliopogon spp. 3 cratered indet.), Tret (Tretopleura weijica sp. inc.), Plat (Platylistrum subviridum sp. inc.), Caul (Caulophacus spp. indet.), Amph (Amphidiscella spp. indet.); Anthozoa: Kera1 (Keratoisididae spp. 1 unbranched indet.), Kera2 (Keratoisididae spp. 2 branched indet.), Ramu (Ramuligorgia militaris), Nare (Narella spp. indet.), Chry (Chrysogorgia spp. indet.), Umbe (Umbellula spp. indet.); Crinoidea: Pent (Pentametrocrinidae spp. indet.), Ante (Antedonidae spp. indet.), Thal (Thalassometra electrae sp. inc.), Guil (Guillecrinus spp. indet.); Ophiuroidea: OpDef (Ophioplinthaca defensor sp. inc.), OpDry (Ophiocamax drygalskii sp. inc.); Asteroidea: Bris (Brisingida spp. indet.); Echinoidea: Ples (Plesiodiadema spp. indet.); Holothuroidea: Enyp (Enypniastes eximia); Decapoda: Shri (Shrimps).

located on the eastern slopes of the Weixie Seamount (Fig. 4, M3,  $10.0\,\%$  of WJS samples). (3) Aggregations of unstalked crinoids (Pentametrocrinidae spp. indet.), always attached to rocky substrates, were mainly located in the southwestern parts of the WJS (Fig. 4, M4,  $24.2\,\%$  of WJS samples). The two assemblages of glass sponge aggregations observed only in the WJS shared similar environmental characteristics, occurring on moderately hard to hard substrates in moderately to highly elevated areas at depths around  $2350\,$ m, while the latter (M3) preferred to occur in the areas with stronger current. The crinoid aggregations were found at shallower depths of  $1550-1750\,$ m, on mixed to moderately hard substrates in moderately elevated areas.

The other four assemblages were distributed in both seamounts. (1) Aggregations characterized by small ophiuroids (*Ophioplinthaca defensor* sp. inc.), along with two morphospecies of unstalked crinoids (*Thalassometra electrae* sp. inc., Pentametrocrinidae spp. indet.), were observed on the slopes of the CWS at depths about 2500 m (Fig. 4, M5,

4.2 % of CWS samples) and mainly in the southwestern parts of the WJS at depths about 1800 m (13.0 % of WJS samples). (2) Aggregations of columnar sponges (*Poliopogon* spp.1 columnar indet. and *Poliopogon* spp.3 cratered indet.) were mainly located on the southern slopes of the Caiqi Seamount (Fig. 4, M6, 16.4 % of CWS samples) and in the southwestern parts of the WJS (8.7 % of WJS samples). (3) Aggregations characterized by whip-like octocorals (Keratoisididae spp. 1 unbranched indet.) were located on the slopes of both the CWS (Fig. 4, M7, 7.4 % of CWS samples) and WJS (6.1 % of WJS samples). (4) Aggregations represented by a few small sea urchins (*Plesiodiadema* spp. indet.) were located around the summits of the CWS (Fig. 4, M8, 4.8 % of CWS samples) and in the northern summits of the WJS (4.3 % of WJS samples).

It should be noted that the percent of unclassified samples was higher in the CWS at 54.0 %, compared to 28.6 % in the WJS. This implies that the CWS may harbor several distinct, small-scale aggregations of benthic

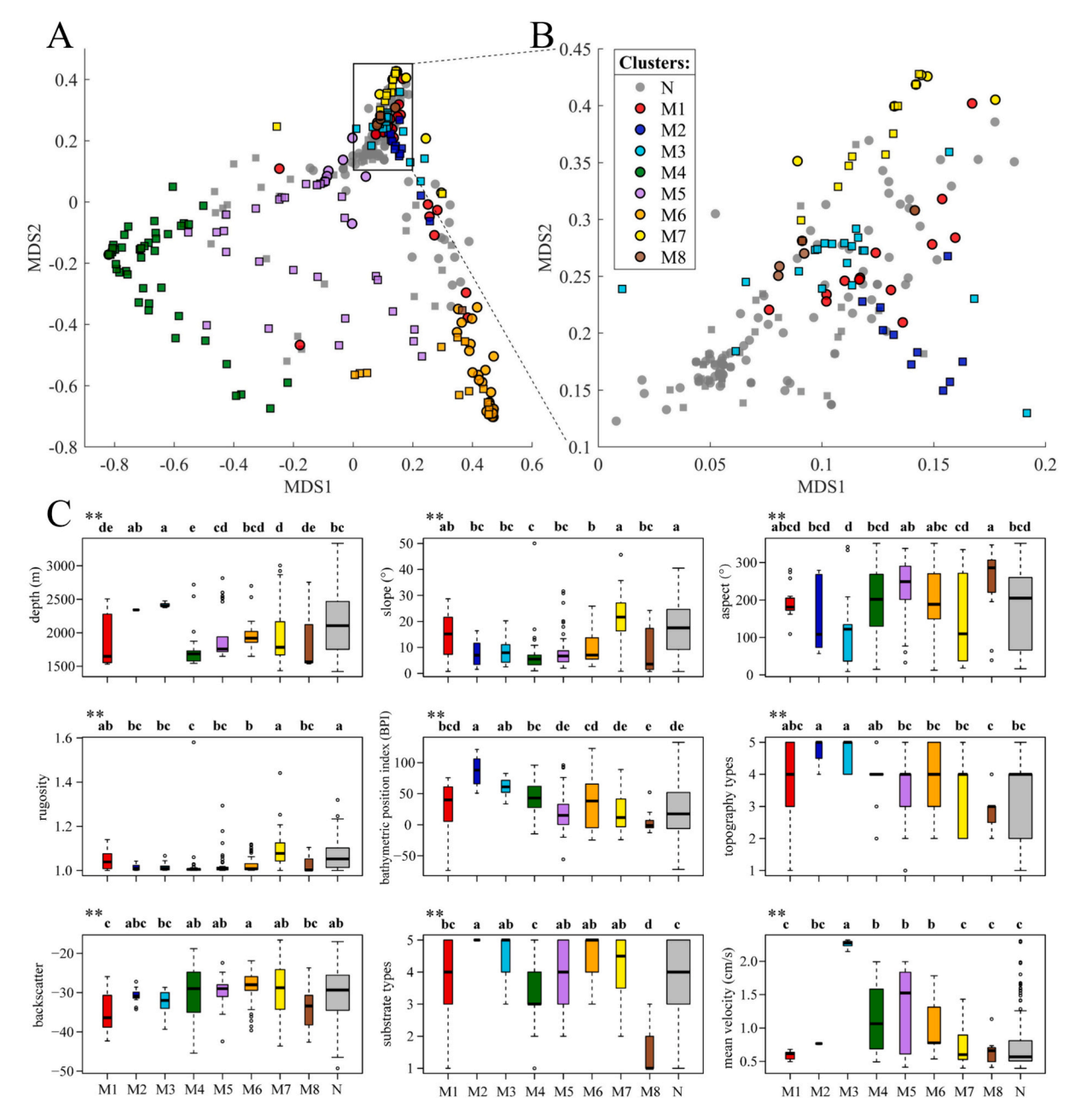


Fig. 3. Multidimensional scaling (MDS) ordination plot of the noise clustering (A) based on the megabenthic data, with the partial close-up (B), and boxplots of each environmental variable for cluster categories with the Kruskal-Wallis test (C). Samples were divided into eight clusters (labeled as M1–M8) with other 40.0 % unclassified (labeled as N). Circles refer to samples from the Caiwei Seamounts, and squares refer to samples from the Weijia Seamounts.

megafauna that were not captured by the clustering analysis at a broader scale. Four examples of these unclassified, potentially outlier assemblages (Supplementary Fig. 2) from the CWS are worth highlighting. (1) Two sequential samples (Fig. 4, N1, dive JL70) on the northeastern slopes of the CWS at a depth of about 2300 m, with highest linear density of 182 ind./100 m, were characterized by dense aggregations of octocorals of branched Keratoisididae along with unbranched Keratoisididae and Primnoidae (*Narella* spp. indet.). (2) One sample (Fig. 4, N2, dive JL79) together with two nearby samples on the northwestern slopes of the CWS at a depth of about 2900 m, with the second highest linear density of 173 ind./100 m, was dominated by a single octocoral morphospecies of Chrysogorgiidae (*Ramuligorgia militaris*) which was not observed in the WJS. (3) Two sequential samples (Fig. 4, N3, dive JL81) on the western slopes of the CWS at a depth of about 1640 m, with a high linear density of 118 ind./100 m, were characterized by dense

aggregations of a single spoon-like sponge morphospecies (*Platylistrum subviridum* sp. inc.). (4) Two sequential samples (Fig. 4, N4, dive JL76) on the western slopes of the CWS at a depth of about 2700 m, despite lower abundances, were dominated by a single morphospecies of elongated sponges (*Semperella* spp. indet.) which was not observed in the WJS.

## 3.4. Alpha and beta diversity

The abundance and relevant alpha diversity indicators of CWS showed a slight unimodal trend along the depth gradient, while the WJS displayed a more pronounced bimodal trend (Fig. 5A–D). The variance-based total beta diversity index of both seamounts was 0.8821 out of 1.0, which was 0.8798 for the CWS and 0.8280 for the WJS when calculated separately, suggesting a high degree of heterogeneity in the megafaunal

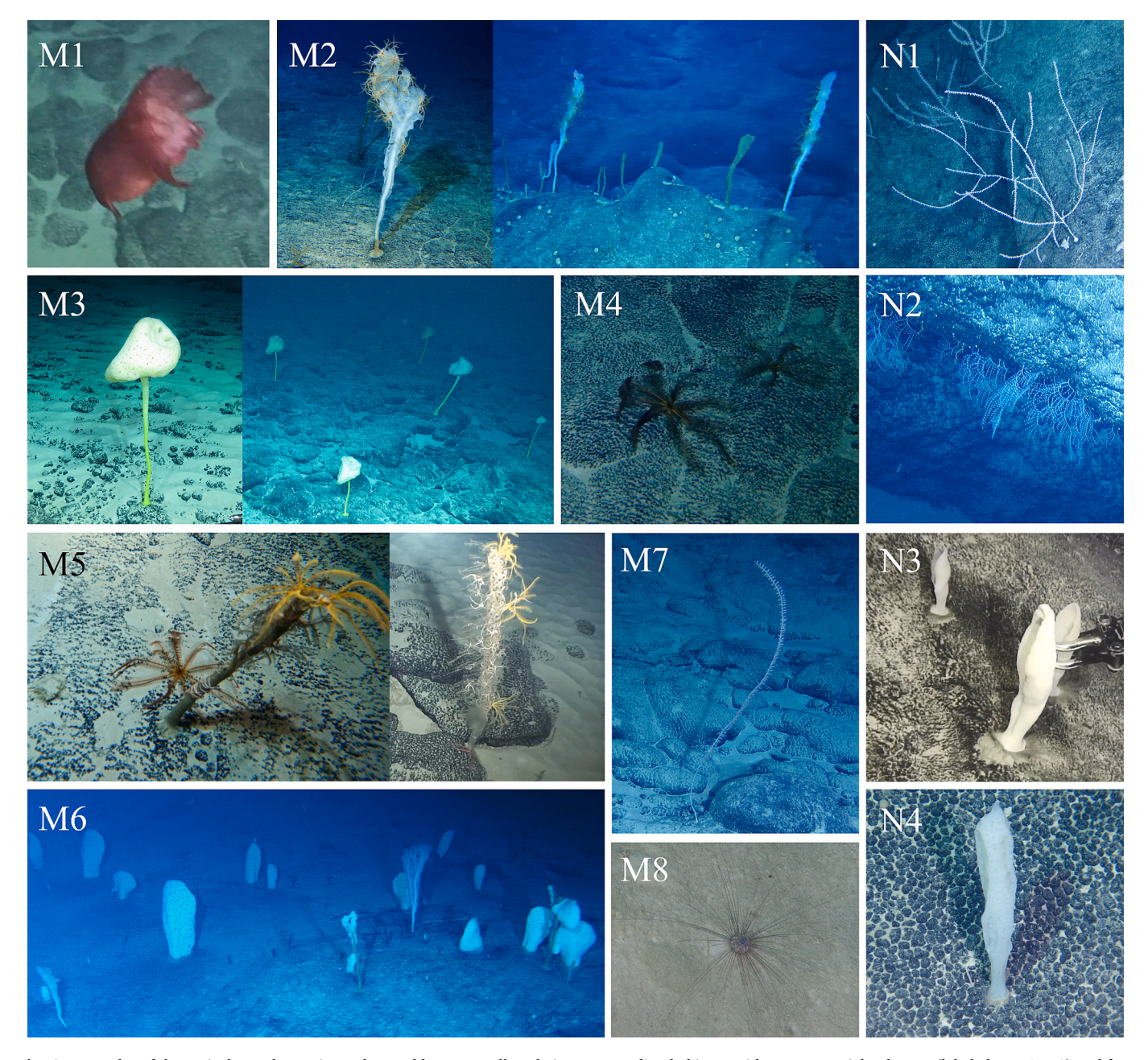


Fig. 4. Examples of the typical morphospecies and assemblages as well as their corresponding habitats, with respect to eight clusters (labeled as M1–M8) and four other unclassified while distinct examples (labeled as N1–N4). M1: Enypniastes eximia; M2: Tretopleura weijica sp. inc., and Antedonidae spp. indet.; M3: Flavovirens hemiglobus sp. inc.; M4: Pentametrocrinidae spp. indet.; M5: Pentametrocrinidae spp. indet., Thalassometra electrae sp. inc., Ophioplinthaca defensor sp. inc., Walteria demeterae sp. inc., and a sponge stalk; M6: Poliopogon spp. 1 columnar indet., Poliopogon spp. 3 cratered indet., and Tretopleura weijica sp. inc.; M7: Keratoisididae spp. 1 unbranched indet.; M8: Plesiodiadema spp. indet.; N1: Keratoisididae spp. 2 branched indet.; N2: Ramuligorgia militaris; N3: Platylistrum subviridum sp. inc.; N4: Semperella spp. indet.

communities across both seamounts. Two abundant and frequently observed morphospecies, Pentametrocrinidae spp. indet. and *Poliopogon* spp.1 columnar indet., contributed greatly to the total beta diversity (Fig. 2H). However, two less abundant and infrequently observed morphospecies, *Plesiodiadema* spp. indet. and *Enypniastes eximia*, also contributed substantially to the total beta diversity (Fig. 2H).

Partitioning of the dissimilarity-based total beta diversity showed the ecological process of species replacement to be dominant (accounting for 60.20 % with a total beta diversity of 0.4639) when using presence-absence data of both seamounts, while the differences in species abundance were slightly dominant (contributing 56.22 % with a total beta diversity of 0.4797) when using abundance data. Similar results were observed when analyzing the presence-absence or abundance

data within each seamount individually. Examining the specific dissimilarity metrics, Jaccard dissimilarity between the two seamounts was generally higher than that within either the CWS or WJS; species replacement was generally lower between the two seamounts compared to within the CWS; richness/abundance differences were generally lower between the two seamounts than within the WJS (Fig. 5E–F). That means, despite that the total dissimilarities were higher between seamounts compared to within a single seamount, the detailed ecological processes may be more pronounced within a single seamount.

## 3.5. Environmental and spatial factors

The dbRDA method with forward selection demonstrated the

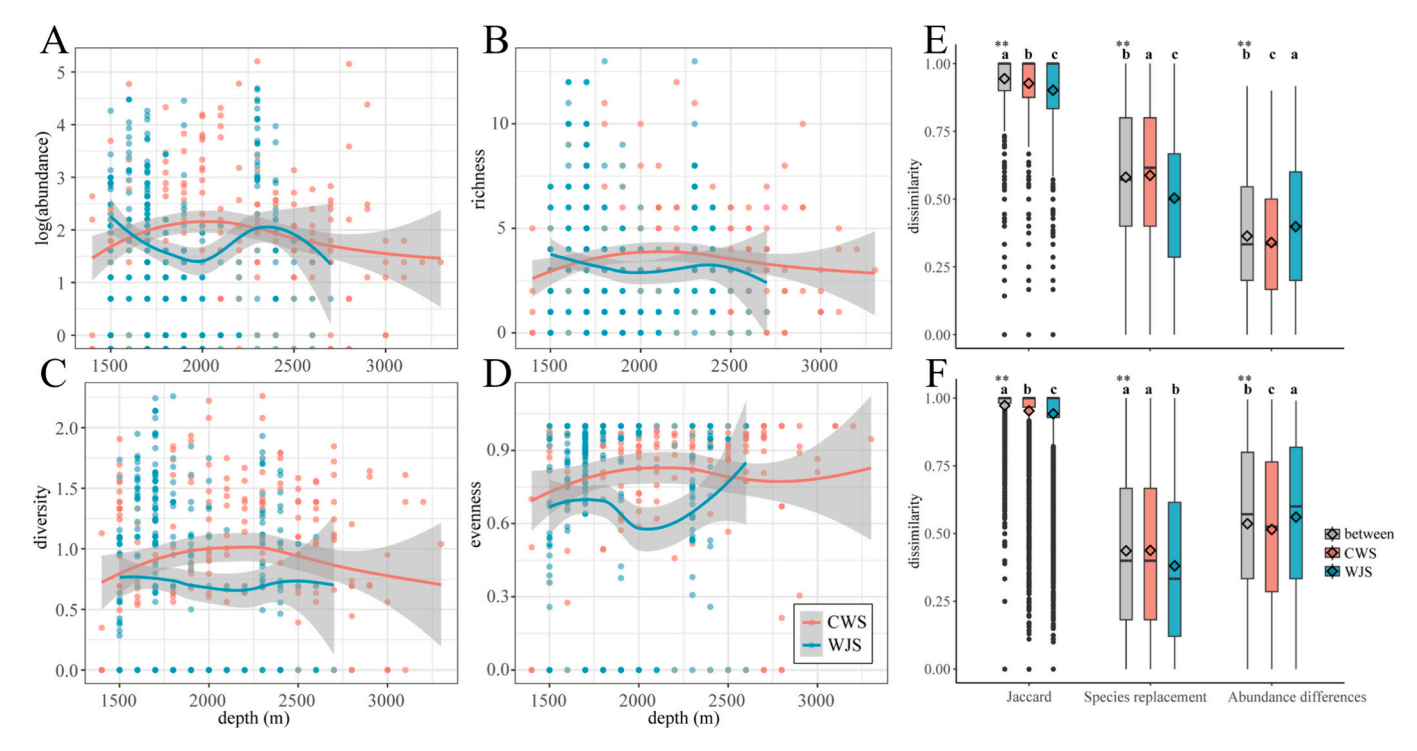


Fig. 5. Change of abundance with a natural logarithm (A) and alpha biodiversity indices, including morphospecies richness (B), Shannon diversity index (C), and Pielou evenness index (D), along the depth gradient (at a resolution of 100 m) by using Loess smoothing method. Boxplots of dissimilarities, based on presence-absence (E) and abundance (F) data, between the Caiwei Seamounts (=CWS) and Weijia Seamounts (=WJS) and within each seamount with the Kruskal-Wallis test. \*\* = p < 0.01; diamonds refer to the average.

Table 1
Results from the Distance-based redundancy analysis (dbRDA) with a forward selection, showing the significant environmental variables (p < 0.05) affecting the Bray-Curtis dissimilarity with  $\log(x+1)$  transformation, Jaccard dissimilarity, species replacement, and abundance/richness difference using species abundance and presence-absence data with one-occurrence species and empty samples removed. BPI = bathymetric position index; \*\* refers to p < 0.01.

	$R_{adj}^2$	Pseudo F- Statistics	Depth	Aspect	Slope	Curvature	Rugosity	BPI	Topography	Substrate	Backscatter	Velocity
a) Species abundance data												
Bray-Curtis dissimilarity (log)	0.0441	2.21**	0.002	0.002	0.002	0.032	0.002	0.002	0.002	0.002	0.002	0.002
Jaccard dissimilarity	0.0771	3.06**	0.002	0.002	0.002	0.012	0.002	0.002	0.002	0.002	0.002	0.002
Species replacement	0.0002	1.03**	0.002	0.002	\	\	\	\	\	\	\	\
Abundance difference	0.0117	1.62**	\	\	0.001	\	\	0.001	\	0.002	\	0.001
b) Presence-absence data												
Bray-Curtis dissimilarity	0.0446	2.22**	0.002	0.002	0.002		0.002	0.002	0.006	0.002	0.002	0.002
Jaccard dissimilarity	0.0995	3.72**	0.002	0.002	0.002	0.026	0.002	0.002	0.002	0.002	0.002	0.002
Species replacement	0.0007	1.02**	0.002		0.002		0.002		0.002	0.010	\	0.004
Richness difference	0.0041	1.21**	\	0.027	\	\	\	0.001	\	0.001	\	0.001

correlation between community structure and at least ten environmental variables, including depth, slope, aspect, rugosity, curvature, BPI, topography types, backscatter, substrate type, and mean velocity (Table 1). For a single seamount, the community structure in the CWS was correlated with at least eight environmental variables, excluding rugosity or topography types. In the WJS, the community structure was correlated with at least eight variables, excluding aspect or backscatter. The ordination plots of dbRDA are shown in Fig. 6A–B. Further hierarchical and variation partitioning of environmental variables (Fig. 6C) (when abundance data used) showed that substrate types made greater contribution to the total explained variation in community structure. Depth explained a much greater proportion of the variation in the WJS compared to the CWS.

The first three principal component axes explained 51.9 % of the total variance (Fig. 6A–B). Based on the length and collinearity of the vectors, mean velocity and BPI played important roles in the distribution

of samples along the first axis. Depth was an important factor along the second axis. Slope and rugosity were important variables across the first three axes. When projected onto the plane formed by the first two axes, the vectors for depth and BPI were nearly orthogonal, indicating these two variables were largely independent in explaining the sample distribution. In terms of the two discrete environmental variables (topography and substrate types), the extent of highly elevated areas with hard substrates was positively correlated with sample scores along the first axis, but negatively correlated with sample scores along the second axis. The extent of hard substrates was negatively related to sample scores along the third axis, while the extent of soft and moderately soft substrates, as well as flat areas, was opposite. The extent of depressed and moderately depressed areas was negatively related to sample scores along the first axis. The extent of mixed substrates and moderately elevated areas was positively related to sample scores along the second axis.

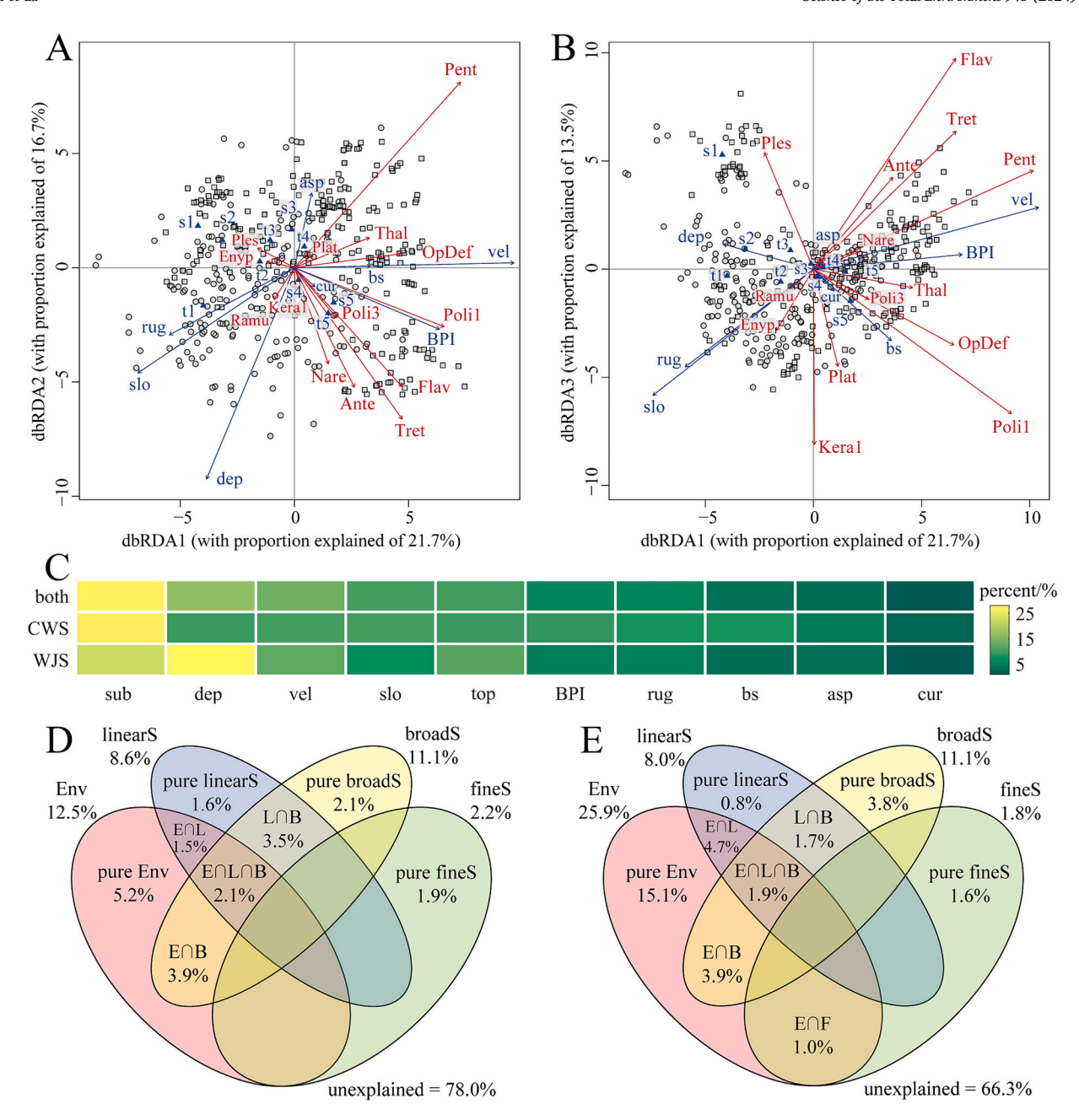


Fig. 6. Plot of the distance-based redundancy analysis (=dbRDA) with forward selection taking the first and second axes as the abscissa and ordinate (A) or taking the first and third axes as the abscissa and ordinate (B). Bray-Curtis dissimilarity with natural log(x + 1) transformation, species abundance data, and a 100 m sample length were used. Heatmap of hierarchical and variation partitioning of environmental variables for dbRDA (C). Distinct morphospecies (in red) are shown. Hexactinellida: Poli1 (Poliopogon spp. 1 columnar indet.), Flav (Flavovirens hemiglobus sp. inc.), Poli3 (Poliopogon spp. 3 cratered indet.), Tret (Tretopleura weijica sp. inc.), Plat (Platylistrum subviridum sp. inc.); Anthozoa: Ramu (Ramuligorgia militaris), Nare (Narella spp. indet.), Keral (Keratoisididae spp. 1 unbranched indet.); Crinoidea: Pent (Pentametrocrinidae spp. indet.), Ante (Antedonidae spp. indet.), Thal (Thalassometra electrae sp. inc.); Ophiuroidea: OpDef (Ophioplinthaca defensor sp. inc.); Echinoidea: Ples (Plesiodiadema spp. indet.); Holothuroidea: Enyp (Enypniastes eximia). Environmental variables (in blue) include substrate (sub or s) types, depth (dep), velocity (vel), slope (slo), topography (top or t) types, bathymetric position index (BPI), rugosity (rug), backscatter (bs), aspect (asp), and curvature (cur). Five types of topography include depressed areas (t1), moderately depressed areas (t2), flat areas (t3), moderately elevated areas (t4), and highly elevated areas (t5). Five categories of substrates include soft (s1), moderately soft (s2), mixed (s3), moderately hard (s4), and hard (s5). Circles refer to the samples from the Caiwei Seamounts (=CWS), and squares refer to the samples from the Weijia Seamounts (=WJS). Venn diagram of the variation partitioning in the CWS (D) and WJS (E), respectively, showing the contributions of environmental (labeled Env or E) and spatial factors, including the linear spatial trend (labeled linearS or L) and broad-scale (labeled broadS or B) and fine-scale (labeled fineS o

In the first quadrant formed by the first two axes, the morphospecies Pentametrocrinidae spp. indet. played an important role, which was positively correlated with *Ophioplinthaca defensor* sp. inc., *Thalassometra electrae* sp. inc., a stalked crinoid (*Guillecrinus* spp. indet.), and *Ophiocamax drygalskii* sp. inc. These assemblages, dominated by crinoids and ophiuroids, showed a significant positive correlation with velocity, but negative correlation with depth, slope, and rugosity. They were

distributed in moderately elevated area with mixed or moderately hard substrates and were mainly associated with samples from the WJS. These features were consistent with the M4 and M5 clusters. In the fourth quadrant formed by the first two axes, several morphospecies of glass sponges, including *Tretopleura weijica* sp. inc., *Flavovirens hemiglobus* sp. inc., *Poliopogon* spp.1 columnar indet., *Poliopogon* spp.3 cratered indet., and *Caulophacus* spp. thin indet., along with unstalked

crinoids of Antedonidae spp. indet. attached to *Tretopleura weijica* sp. inc., played important roles. These glass sponge-dominated assemblages, showed a significant positive correlation with BPI, velocity, and depth. They were preferentially distributed in highly elevated areas with hard or moderately hard substrates. The morphospecies of *Tretopleura weijica* sp. inc. and *Flavovirens hemiglobus* sp. inc. were positively related to the third axis and largely correlated with WJS samples. These features were consistent with the M2 and M3 clusters. In contrast, the morphospecies of *Poliopogon* spp.1 columnar indet. and *Poliopogon* spp.3 cratered indet. were negatively related to the third axis, consistent with the M6 cluster.

In the plane formed by the first and third axes, a morphospecies of octocorals, unbranched Keratoisididae along with branched Keratoisididae, showed negatively collinear with the third axis and were affected by slope and rugosity, consistent with the M7 cluster. The morphospecies of *Enypniastes eximia* was projected in the third quadrant formed by the first and third axes, which was positively correlated with slope and rugosity but negatively correlated with velocity, consistent with the M1 cluster. The morphospecies of *Ramuligorgia militaris* exhibited similar features. The morphospecies of *Plesiodiadema* spp. indet. was projected in the second quadrant formed by the first and third axes, relevant to flat areas with soft and moderately soft substrates, consistent with the M8 cluster.

Spatial analysis showed that environmental and spatial variables explained 22.0 % and 33.7 % of the variation in the megafaunal community located in the CWS and WJS, respectively (Fig. 6D-E). The environmental variables explained less in the CWS (12.5 %) compared to the WJS (25.9 %). Of them, 5.2 % and 15.1 % were not spatially structured and associated only with local environmental conditions in the CWS and WJS, respectively. The spatial variables showed similar levels of variation explained in the two seamounts. The variation explained by the linear trend was about 8 % in both the CWS and WJS, and the common part of this linear trend shared with the environmental variables was 1.5 % and 4.7 %, respectively. This common fraction suggests that the linear gradient of the environmental variables produced a similar linear trend in the species data. The spatial variation at broad and fine scales was about 11 % and 2 %, respectively, in both the CWS and WJS. Additionally, for the two seamounts, the variation common to broad-scale spatial and environmental variables was 3.9 % in both seamounts. In the CWS, the broad-scale spatial variable was significantly related to at least eight environmental variables, excluding aspect or topography types; the fine-scale spatial variable was related to slope, rugosity, topography types, and backscatter. In the WJS, the broad-scale spatial variable was significantly related to at least six environmental variables, excluding rugosity, BPI, topography types or velocity; the fine-scale spatial variable was related to depth, slope, curvature, BPI, topography types, and velocity.

## 4. Discussion

## 4.1. Similar density, richness, and megafaunal lists between seamounts

The survey results indicated that the CWS had a density of 12.3 ind./ 100 m with a total of 70 morphospecies of megafauna observed; similarly, the WJS showed a density of 12.3 ind./100 m with a total of 66 morphospecies. Compared to other bathyal features with cobalt-rich crusts, the abundance observed in this study was far lower than that reported for the Necker Ridge, which had comparable sampling depths of 1400–2000 m (Morgan et al., 2015), as well as the RGR, which had shallower sampling depths of 600–2000 m (Corrêa et al., 2022). This lower abundance observed in the current study was despite the use of similar video observation sampling efforts across these studies, as summarized in Supplementary Table 5. Although the specific number of megabenthic individuals was not reported for the Hawaiian Seamount Chain, the >300 morphospecies documented in the cobalt-rich crust seamounts at 700–2000 m depths (Schlacher et al., 2014) suggests a

potentially high abundance that may be more comparable to the Necker Ridge adjacent to it. The overall lower abundance of megafauna observed in these two cobalt-rich crust seamounts was consistent with the previous case study on the Cross Seamount (Grigg et al., 1987). Thus, more comprehensive case studies on the benthic fauna of seamounts are essential to make definitive statements about whether benthic megafauna occur at greater or lower density in the cobalt-rich crust region (Schlacher et al., 2014). Moreover, the number of morphospecies documented in these two seamounts was comparable to that reported for the RGR (83 morphospecies; Corrêa et al., 2022) as well as the Necker Ridge (around 70 morphospecies; Morgan et al., 2015), despite the disparities in megafaunal density. Accordingly, the previous statement of a lower number of taxa in cobalt-rich crust seamount regions (Grigg et al., 1987) was not supported by the findings of this study. This earlier view had been rejected by most subsequent case studies as well (Morgan et al., 2015; Schlacher et al., 2014).

The megafaunal taxa observed in the two seamounts shared five phyla, including Porifera, Cnidaria, Echinodermata, Arthropoda, and Chordata, among which the first three phyla collectively contributed >90 % of the total abundance observed in this study, consistent with the cases reported for other cobalt-rich crust regions, such as the RGR (Corrêa et al., 2022) and Necker Ridge (Morgan et al., 2015). At the level of morphospecies, the richness similarity index between the two seamounts, which are located approximately 350 km apart, was 69.1 %, which increased to 77.7 % when the morphospecies only observed once was excluded, indicating a high degree of overlap in the megafaunal composition between these two cobalt-rich crust seamounts despite their geographic separation. For the seamounts located either inside or outside the cobalt-rich crust regions, there were 135 distinct taxa that were common across these areas at depths of 700-2000 m, out of a total of >500 taxa (Schlacher et al., 2014). This resulted in a richness similarity index of about 53 % between the seamounts inside and outside the cobalt-rich crust regions, despite a maximum geographic separation of up to 2200 km between the seamounts. As noted by Clark et al. (2012), seamounts are generally not ecologically isolated systems, and often have assemblages of similar species composition to those found in adjacent deep-sea habitats, which may also apply to the cobalt-rich crust seamounts.

In terms of the biological traits of megabenthos, filter and suspension feeders dominated in both seamounts (Fig. 2E). It is a typical characteristic of seamount megafaunal communities, as these feeding strategies are known to benefit from the accelerated hydrodynamic conditions commonly found on seamounts (Genin et al., 1986; Perez et al., 2018). Thus, the deep-water seamount fauna are widely recognized to be easily disturbed by sediment plumes caused by mining activities. In terms of movement mode, the sessile fauna dominated in the CWS, while the WJS exhibited a slightly higher proportion of mobile fauna compared to sessile fauna; the swimming fauna, including fishes, shrimps, and swimming holothurian, were less observed in the two deep-water seamounts (Fig. 2C). The dominance of sessile organisms is a key characteristic to identify vulnerable indicator taxa on seamounts. Sessile fauna have a higher potential to provide biogenic habitat structures but are also more directly susceptible to physical disturbance. While seamounts are typically dominated by hard substrates that favor the sessile taxa, such as corals, sponges, and stalked crinoids, the degree of sessile dominance observed in these deep-water seamounts may not be as pronounced as in other seamount environments. It implies that in addition to the sessile habitat-forming taxa commonly recognized as vulnerable indicators, the non-sessile organisms, such as unstalked echinoderms, should also be carefully investigated. Their vulnerability can be assessed based on the uniqueness or rarity of the species, as well as their functional significance to the overall seamount ecosystem (Morato et al., 2018; Watling and Auster, 2021). Given the currently limited knowledge on deep-water seamount ecosystems, the aggregation of non-sessile taxa at a small scale or their occurrence as distinct communities could potentially serve as a surrogate indicator to assess their

functional fragility.

## 4.2. Dissimilarity of assemblage composition between deep-water seamounts

Despite the overall similarity in megafaunal lists between the two seamounts, there were great differences in the relative abundances (referring to the faunal composition). Among the three predominant phyla, sponges dominated in the CWS while echinoderms dominated in the WJS, with both phyla contributing around half of the total abundance in their respective seamounts. The megafauna in the CWS and WJS showed a high dominance of a few morphospecies, but the dominant species differed between the two seamounts. In the CWS, a dominant morphospecies of sponge (Poliopogon spp. 1 columnar indet.) was highly more abundant compared to other morphospecies, while a dominant morphospecies of unstalked crinoid (Pentametrocrinidae spp. indet.) was extremely more abundant in the WJS. The Necker Ridge also provides an illustrative example of the significant difference in dominating morphospecies that can occur between nearby deep-sea features. The southern and northern pinnacles of the Necker Ridge, separated by a maximum distance of 117 km, were dominated by unstalked crinoids (the Family Charitometridae) and octocorals (the Families Keratoisididae and Chrysogorgiidae), respectively (Morgan et al., 2015). These dominating morphospecies were also commonly observed in this study, but less dominant. In addition, the transition between the crinoiddominated communities in the southern Necker Ridge and the coraldominated communities in the north was observed to be a gradual change, rather than an abrupt community shift (Morgan et al., 2015). Thus, a biological investigation on the seamount located between the CWS and WJS, named Fedorov Seamount in the GEBCO (Fig. 1B), would be valuable to better understand the population connectivity and spatial succession of communities along the Magellan Seamount Chain.

The great differences observed in the relative abundances of benthic megafauna contributed to the significant variations in assemblage composition between the two seamounts to a certain extent. One of the most dominant morphospecies, the unstalked and independently living crinoid (Pentametrocrinidae spp. indet.), was extremely more abundant in the WJS, and accordingly resulted in a distinct assemblage featured by its prominent aggregations in the WJS. Two other distinct assemblages only observed in the WJS, including aggregations of a blade-like sponge (Tretopleura weijica sp. inc.) and aggregations of a stalked sponge (Flavovirens hemiglobus sp. inc.), were also resulted from the higher local abundance of their representative morphospecies within the WJS, although not the overall dominance in the study area. For the distinct assemblage observed only in the CWS, it was represented by a morphotype of preferentially swimming holothurians, Enypniastes eximia, which was not observed in the WJS. The movement capability of preferentially swimming holothurians implies a higher dispersal potential in the deep sea (Baco et al., 2016). Their occurrence and aggregation observed solely in the CWS may be attributed to the influences of relatively small environmental differences on their larval settlement or juvenile growth. According to the results of noise clustering, the similarity index of assemblages between the two seamounts was initially calculated as two-thirds. However, when also considering the other 40 %unclassified samples, qualitative analyses showed that there were at least four additional distinct assemblages occurring at small scales within the CWS (Fig. 4). Taking these small-scale distinct assemblages into account, the similarity index of assemblages between the two seamounts decreased to approximately 50 %. This suggests that higher spatial resolution is needed to capture the fine-scale spatial variation of megafaunal distribution to better understand the full suite of distinct communities within the seamount environments.

Furthermore, the representative morphospecies comprising each of these distinct assemblages may not necessarily be the same megabenthic morphospecies that aggregate in other seamounts that have been studied. The specific assemblage compositions observed in this study appear to be distinct from the typical assemblages reported for other seamounts. For example, a hexactinellid sponge morphospecies (*Advhena magnifica* sp. inc.) was reported to aggregate in a northern Mid-Pacific seamount at around 2400 m depth (Castello-Branco et al., 2020), and an octocoral morphospecies (*Chrysogorgia* spp. indet.) was observed to aggregate on the Necker Ridge at around 1800 m depth (Morgan et al., 2015), both of which were less commonly observed in this study. Similarly, the cobaltrich crust habitats in the RGR were found to be dominated by the sponge aggregations of the hexactinellid *Sarostegia oculata* (Hajdu et al., 2017), which have rarely been reported elsewhere (Corrêa et al., 2022). Further biological investigations would be needed to determine whether these distinct communities imply a high affinity for cobalt-rich crust habitats, or if they primarily result from the inherent heterogeneity of local habitats and source populations at the regional scales.

#### 4.3. High patchiness of community structure throughout seamounts

The calculated values of total beta diversity index based on variance were high in both seamounts, with a value of 0.8798 for the CWS and 0.8280 for the WJS, out of a maximum of 1.0. When compared to shallower seamounts, the benthic megafauna in the Annan Seamount of Equatorial Atlantic exhibit an index of 0.92 across a bathymetric gradient of 200-2730 m (Victorero et al., 2018). Similarly, the North Pacific seamount Mokumanamana shows values of 0.90-0.95 along the depth gradient of 200-700 m and 0.81-0.88 between different sides (Morgan et al., 2019). The findings suggest a considerable spatial variation in the megafaunal community structure throughout both shallower and deeper seamounts. Likewise, studies have reported a substantial changeover in diversity and community structure within cobalt-rich crust regions (Corrêa et al., 2022; Morgan et al., 2015; Schlacher et al., 2014), aligning with the general patterns observed in the deep sea (Levin et al., 2001; Rex and Etter, 2010). Among the distinct assemblages observed in this study, the samples featuring a few small sea urchins (Plesiodiadema spp. indet.), distributed in both seamounts, made significantly higher contributions to the total beta diversity. It suggests that the rarer species may form ecologically unique communities, which could in turn to improve the rate of faunal turnover (McClain and Lundsten, 2015). Nevertheless, for the morphospecies with high abundance, including Pentametrocrinidae spp. indet. and Poliopogon spp.1 columnar indet., also contributing greatly to the beta diversity, their respective assemblages showed relatively lower contributions to the overall beta diversity. That means, the spatial variability of community structure within these deep-water seamounts may exhibit significantly different characteristics compared to the patterns of overall biodiversity.

The partitioning of the dissimilarity-based total beta diversity in both seamounts revealed that it was dominated by species replacement (60.20 %) for presence-absence data, while slightly dominated by abundance differences (56.22 %) for abundance data. This suggests that there were significant differences in both species composition and abundance among the different samples (on a scale of 100 m) in the study area, while the gain and loss of species were less significant. In addition to the high spatial variation observed in the community structure, it implies that the spatial distribution of megabenthic communities in the seamounts presents a discontinuous and patchy/mosaic pattern, as reported in previous studies (Clark et al., 2012; McClain et al., 2010; Morgan et al., 2015; Perez et al., 2018). The relatively high degree of species replacement was mainly due to environmental filtering (Moraitis and Karakassis, 2020), which plays a stronger role than biotic interactions in structuring communities in areas subjected to high abiotic stress (Sommer et al., 2014). The species replacement rate is regarded as a function of the ecological tolerance, or niche breadth, of the individual species (Legendre, 2014). This suggests that the observed community structure is the result of different levels of ecological tolerance of individual species to environmental conditions or disturbances (Fajardo et al., 2018; Moraitis and Karakassis, 2020), especially in the

deep-sea environment with less biotic competition. Consequently, distinct assemblages may occur within a relatively narrow range of environmental niche breadth (Granot and Belmaker, 2020). This spatial pattern, where high beta diversity is mainly driven by species replacement rather than species loss, has been previously noted in the highly fluctuant marine benthic environments (Moraitis and Karakassis, 2020 and references therein). Despite the relatively homogeneous environments overall in the deep sea, at the local scale, changes in environmental conditions mainly caused by terrain, current, and biogenic substrates also result in significant species turnover in the seamounts.

For different spatial scales, the Jaccard dissimilarity between the two seamounts showed that the index was significantly higher than that within the CWS or WJS, and the species replacement between the two seamounts was generally higher than that within the WJS (Fig. 5E-F), consistent with a previous case study (Perez et al., 2022). Contrarily, within the CWS, a higher level of species replacement was showed, suggesting the relative importance of environmental filtering within the CWS compared to that between the two seamounts and especially within WJS. Nevertheless, the spatial analysis showed that the variation in community structure explained by environmental variables was quite lower in the CWS compared to the WJS, while the spatial variation at fine scales was slightly higher. It suggests that biological investigations at a finer scale in the CWS are needed to include the effects of microhabitats. In addition, the relative importance of richness and abundance differences between the two seamounts compared to that within the CWS was present, contrary to the patterns in the WJS. It implied that there was a higher difference in niche diversity available for the species (Legendre, 2014) and resources available for individual organisms among the samples between the two seamounts than within the CWS.

# 4.4. Interplay of multiple biotic and abiotic factors strengthening biological patchiness

The spatial distribution of megabenthic communities presents a discontinuous and patchy/mosaic pattern. The results of the dbRDA with forward selection showed that this pattern of megabenthic assemblages and their spatial variations in this study were impacted by at least ten environmental variables, including depth, slope, aspect, rugosity, curvature, BPI, topography types, backscatter, substrate, and mean velocity of near-bottom currents.

The nature of substrates directly impacts species occurrence, particularly for sessile or sedentary invertebrates, due to the influence of substrate features on the attachment methods and feeding habits. An obvious example from this study is the restricted occurrence of a few small echinoids (Plesiodiadema spp. indet.) in the sandy substrates, especially on the sedimentary plateaus of these two typical guyots, since that the sandy and flat seafloor at bathyal depths is beneficial for echinoid spawning (Young et al., 1992). Meanwhile, substrate types can reflect the biotic tolerance to sedimentation. For instance, despite their filter-feeding habits and attachment to hardgrounds, stalked crinoids have been observed to inhabit substrates with higher sediment coverage compared to octocorals, implying a decreased sensitivity of crinoids to sedimentation compared to octocorals (Morgan et al., 2015). This is likely due to the differences in their filter-feeding mechanisms, as corals use mucus-covered polyps while crinoids use specially arrayed tube feet (Meyer, 1979). The backscatter intensity can serve as an indicator of substrate characteristics, as it has been show to correlate significantly with grain size, volume heterogeneity, and interfacial roughness of the seabed substrates (Wang et al., 2021). While the explanatory power of backscatter may be limited in present results, its utility could potentially improve if the variable of substrate types is excluded from the analysis.

It is generally regarded that the habitat-forming taxa tend to preferentially occur in locations with accelerated currents, which can increase food availability in these regions. The glass sponges observed in this study, including blade-like *Tretopleura weijica* sp. inc., stalked *Flavovirens hemiglobus* sp. inc., and columnar or massive *Poliopogon* species,

which are large in body size and serve as the main habitat-forming fauna, showed a significantly positive correlation with current velocity. The assemblages formed by these glass sponges exhibited distinct patterns. The aggregations dominated by Flavovirens hemiglobus sp. inc. occurred in areas with much stronger near-bottom currents and a certain degree of sediment coverage. In contrast, the assemblage dominated by Tretopleura weijica sp. inc. was found in areas with relatively weaker currents and less sediments compared to the other sponge-dominated assemblages. It may be due to the ability of sponges to actively pump water through their choanocytes, allowing them to more effectively trap food particles and adapt to diverse environments with different current velocities (Morgan et al., 2015). Besides feeding habits, the movement methods of invertebrates also play a key role in determining their selection of flow conditions. The holothurian Enypniastes eximia, for instance, was observed to occur in locations with weaker currents. It may be because their preferentially swimming movement behavior is unable to tolerate strong currents. That is why this kind of holothurians was only observed in the CWS, where the near-bottom currents were widely weaker, while the WJS experienced significantly stronger currents. Topographic variables such as BPI and topographic types are often identified as effective indicators of topography-induced currents, which can be key drivers of megabenthic communities on deep-sea seamounts (Genin et al., 1989; Rogers, 2018; Shen et al., 2021). Nevertheless, despite the significant difference in current velocity observed between the two seamounts in this study, there was no statistically significant difference in BPI or topographic types between them. In addition to the similar guyot shape and summit depths (lower than 1450 m) shared by the two seamounts, this finding underlines the complex and nuanced relationship between seamount morphology and the resulting hydrodynamics (Jiang et al., 2021).

In contrast to the glass sponges, cold-water corals and their associated assemblages did not show statistically significant correlation with current velocity in this study. Previous research has reported that reefbuilding cold-water corals in Area Beyond National Jurisdiction (ABNJ) are primarily scleractinian corals, and they are largely distributed in geomorphological features with steep topographies, occurring at depths ranging from 218 to 5567 m with an average of 1058 m (Wagner et al., 2020). However, these reef-building corals were absent from the studied seamounts. Moreover, the cold-water corals present in the studied seamounts did not form extensive aggregations. Only small patches with dense octocorals were observed, dominated by morphospecies such as the unbranched or branched Keratoisididae, Narella spp. indet., or Ramuligorgia militaris, which are small or have a relatively soft texture. This suggests a more limited role of cold-water corals in forming extensive structural habitats in this study area compared to glass sponges. These findings may be due to limitations in the chemical conditions, such as the calcite and aragonite saturation state, which has been identified as one of the most important factors in determining the suitability of cold-water coral habitats (Davies and Guinotte, 2011; Yesson et al., 2012). The cold-water corals observed in this study area showed a positive correlation with slope and rugosity. While their aggregations were limited in scale, this may be a result of the effects of microhabitat features, such as the generally even topography interspersed with boulders. These microhabitats may provide suitable conditions and increased food availability even at the meter scale, playing an important role in shaping the discontinuous and patchy distribution patterns of megabenthic communities throughout the two seamounts.

It should be noted that although depth was one of the significant factors impacting the distribution of megabenthic communities in this study, a regular pattern of biodiversity along the depth gradient was absent. Instead, two peaks of abundance and alpha diversity were observed at bathyal depths of approximately 1700 m and 2300 m in the WJS, which were caused by distinct assemblages (Shen et al., 2021). It implies that depth may represent underlying environmental conditions and its effects on megabenthic community distribution especially in the deep-water seamounts need further investigations. The dbRDA showed

that although depth was not a significant factor in driving the ecological processes of richness and abundance differences, it did play a crucial role in promoting the species replacement (Table 1). This case study was therefore consistent with the previous statement that there was no significant relationship between alpha diversity and depth, but substantial changes in assemblage structure occurred along the bathymetric gradient (Bridges et al., 2022).

#### 5. Conclusion

This case study on the megabenthic community structure of two seamounts in the northwestern Pacific Ocean indicated that the deepwater seamounts, which are covered by cobalt-rich ferromanganese crusts, can support diverse and moderately abundant megafauna with multiple distinct assemblages. The megabenthic communities of these two deep-water seamounts, with comparable environmental conditions, exhibited similarities in overall density, richness, and faunal lists, while dissimilarities in the relative abundance of taxa and assemblage composition. Hexactinellid sponges and octocorals were the dominant habitat-forming taxa in the CWS, while echinoderms, especially of crinoids and ophiuroids, dominated in the WJS. Nevertheless, the WJS was also featured by the occurrence of several localized aggregations of hexactinellid sponges. Those distinct aggregations of habitat-forming taxa in the CWS often occurred within a range of just a few hundred meters. It indicated that the spatial distribution of megabenthic communities presented a discontinuous and patchy pattern throughout both of the deep-water seamounts. This patchiness was driven by the interaction of multiple environmental factors, including substrate and topographic features, near-bottom currents, microhabitat features, and other chemical conditions. Thus, due to the heterogeneous habitats across the seamounts, there was no gradual, depth-related change observed in terms of abundance, richness, or species turnover in the two seamounts, despite the statistically significance of depth in structuring the overall community structure.

The distinct distribution of megabenthic communities on these seamounts implies that the exploitation of cobalt-rich ferromanganese crusts will not only likely lead to biodiversity loss but may also completely disrupt the existing community patches. Besides the assemblages dominated by habitat-forming taxa like sponges and corals, the distinct assemblages aggregated by echinoderms should also be protected seriously due to their ecological significance in the deep-water seamount ecosystems. The high degree of habitat heterogeneity and biological patchiness present on these deep-water seamounts adds complexity to the spatial placement of protected area network in consideration of spatial configuration of habitats and patterns of species distributions. Compared to relying solely on bathymetric gradients, habitat classification based on substrate and topographic features may be a more applicable approach for indicating megabenthic community distribution on the deep-water seamounts. The results of this case study on the megabenthic community structure of two adjacent seamounts with cobalt-rich crusts can serve as an environmental baseline, providing a crucial reference status for the conservation and management of seamount ecosystems, especially in areas being considered for deep-sea mining.

## CRediT authorship contribution statement

Chengcheng Shen: Writing – review & editing, Writing – original draft, Methodology, Funding acquisition, Formal analysis, Data curation, Conceptualization. Runxuan Yan: Writing – original draft, Software, Formal analysis. Bo Lu: Writing – original draft, Investigation. Zhenggang Li: Writing – original draft, Investigation. Ruiyan Zhang: Writing – original draft, Investigation. Dongsheng Zhang: Writing – review & editing, Resources, Project administration, Conceptualization. Chunsheng Wang: Writing – review & editing, Supervision, Resources, Project administration.

#### **Declaration of competing interest**

The authors declare that they have no known competing financial interests or personal relationships that could have appeared to influence the work reported in this paper.

### Data availability

Data will be made available on request.

## Acknowledgements

We are grateful to all the scientists and crew on the R/V "Xiangyanghong 09", "Haiyangdizhi 6", and "Dayangyihao", as well as the teams of HOV Jiaolong, ROV Haima, and ROV Hailong III, for their dedicated research work and collection of deep-sea materials. We thank the anonymous reviewers for their constructive suggestions. This work was supported by the Laoshan Laboratory (grant number LSKJ202203605); the National Natural Science Foundation of China (grant number 42276132); and the Scientific Research Fund of the Second Institute of Oceanography, MNR (grant number ONYC2303).

## Appendix A. Supplementary data

Supplementary data to this article can be found online at https://doi.org/10.1016/j.scitotenv.2024.173914.

#### References

- Baco, A.R., Etter, R.J., Ribeiro, P.A., von der Heyden, S., Beerli, P., Kinlan, B.P., 2016. A synthesis of genetic connectivity in deep-sea fauna and implications for marine reserve design. Mol. Ecol. 25, 3276–3298. https://doi.org/10.1111/mec.13689.
- Blanchet, F.G., Legendre, P., Borcard, D., 2008. Forward selection of explanatory variables. Ecology 89, 2623–2632. https://doi.org/10.1890/07-0986.1.
- Borcard, D., Gillet, F., Legendre, P., 2018. In: Numerical Ecology with R, second ed. Springer, Verlag, New York.
- Bridges, A.E.H., Barnes, D.K.A., Bell, J.B., Ross, R.E., Howell, K.L., 2022. Depth and latitudinal gradients of diversity in seamount benthic communities. J. Biogeogr. 49, 904–915. https://doi.org/10.1111/jbi.14355.
- Castello-Branco, C., Collins, A.G., Hajdu, E., 2020. A collection of hexactinellids (Porifera) from the deep South Atlantic and North Pacific: new genus, new species and new records. PeerJ 8, e9431. https://doi.org/10.7717/peerj.9431.
- China Ocean Mineral Resources Research and Development Association (COMRA) Office, 2017. Chinese Gazetteer of Undersea Features on the International Seabed. Ocean Press, Beijing, China.
- Clark, M.R., Koslow, J.A., 2007. Impacts of fisheries on seamounts. In: Seamounts: Ecology, Fisheries & Conservation. John Wiley & Sons, Ltd, pp. 413–441. https://doi.org/10.1002/9780470691953.ch19.
- Clark, M.R., Rowden, A.A., Schlacher, T., Williams, A., Consalvey, M., Stocks, K.I., Rogers, A.D., O'Hara, T.D., White, M., Shank, T.M., Hall-Spencer, J.M., 2010. The ecology of seamounts: structure, function, and human impacts. Annu. Rev. Mar. Sci. 2, 253–278. https://doi.org/10.1146/annurev-marine-120308-081109.
- Clark, M.R., Watling, L., Rowden, A.A., Guinotte, J.M., Smith, C.R., 2011. A global seamount classification to aid the scientific design of marine protected area networks. Ocean Coast. Manag. 54, 19–36. https://doi.org/10.1016/j. ocecoaman.2010.10.006.
- Clark, M.R., Schlacher, T.A., Rowden, A.A., Stocks, K.I., Consalvey, M., 2012. Science priorities for seamounts: research links to conservation and management. PLoS One 7, e29232. https://doi.org/10.1371/journal.pone.0029232.
- Corrêa, P.V.F., Jovane, L., Murton, B.J., Sumida, P.Y.G., 2022. Benthic megafauna habitats, community structure and environmental drivers at Rio Grande rise (SW Atlantic). Deep Sea Res. Part Oceanogr. Res. Pap. 186, 103811 https://doi.org/ 10.1016/j.dsr.2022.103811.
- Davies, A.J., Guinotte, J.M., 2011. Global habitat suitability for framework-forming cold-water corals. PLoS One 6, e18483. https://doi.org/10.1371/journal.pone.0018483.
- De Cáceres, M., Font, X., Oliva, F., 2010. The management of vegetation classifications with fuzzy clustering. J. Veg. Sci. 21, 1138–1151. https://doi.org/10.1111/j.1654-1103.2010.01211.x.
- Dray, S., Legendre, P., Peres-Neto, P.R., 2006. Spatial modelling: a comprehensive framework for principal coordinate analysis of neighbour matrices (PCNM). Ecol. Model. 196, 483–493. https://doi.org/10.1016/j.ecolmodel.2006.02.015.
- Fajardo, M., Andrade, D., Bonicelli, J., Bon, M., Gómez, G., Riascos, J.M., Pacheco, A.S., 2018. Macrobenthic communities in a shallow normoxia to hypoxia gradient in the Humboldt upwelling ecosystem. PLoS One 13, e0200349. https://doi.org/10.1371/ journal.pone.0200349.

- Fan, M., Shi, S., Ma, Y., Wang, H., Zhai, J., Zhang, X., Ning, P., 2022. High Resolution Geomorphological Classification of Benthic Structure on the Western Pacific Seamount. Front. Mar, Sci, p. 9.
- FAO, 2009. International Guidelines for the Management of Deep-Sea Fisheries in the High Seas Directives. Food and Agricultural Organization of the United Nations. http://www.fao.org/3/i0816t/10816T.pdf.
- Genin, A., Dayton, P.K., Lonsdale, P.F., Spiess, F.N., 1986. Corals on seamount peaks provide evidence of current acceleration over deep-sea topography. Nature 322, 59–61. https://doi.org/10.1038/322059a0.
- Genin, A., Noble, M., Lonsdale, P.F., 1989. Tidal currents and anticyclonic motions on two North Pacific seamounts. Deep Sea res. Part Oceanogr. Res. Pap. 36, 1803–1815. https://doi.org/10.1016/0198-0149(89)90113-1.
- Goode, S.L., Rowden, A.A., Bowden, D.A., Clark, M.R., 2020. Resilience of seamount benthic communities to trawling disturbance. Mar. Environ. Res. 161, 105086 https://doi.org/10.1016/j.marenvres.2020.105086.
- Gotelli, N.J., Colwell, R.K., 2001. Quantifying biodiversity: procedures and pitfalls in the measurement and comparison of species richness. Ecol. Lett. 4, 379–391. https:// doi.org/10.1046/j.1461-0248.2001.00230.x.
- Granot, I., Belmaker, J., 2020. Niche breadth and species richness: correlation strength, scale and mechanisms. Glob. Ecol. Biogeogr. 29, 159–170. https://doi.org/10.1111/geb.13011.
- Grigg, R.W., Malaboff, A., Chave, E.H., Landahl, J., 1987. Seamount benthic ecology and potential environmental impact from manganese crust Mining in Hawaii. In: Seamounts, Islands, and Atolls. American Geophysical Union (AGU), pp. 379–390. https://doi.org/10.1029/GM043p0379.
- Hajdu, E., Castello-Branco, C., Lopes, D.A., Sumida, P.Y.G., Perez, J.A.A., 2017. Deep-sea dives reveal an unexpected hexactinellid sponge garden on the Rio Grande Rise (SW Atlantic). A mimicking habitat? Deep Sea Res. Part II Top. Stud. Oceanogr., Geo and bio-diversity in the South West Atlantic deep sea: the Iatá-piúna expedition with the manned submersible Shinkai 6500 146, pp. 93–100. https://doi.org/10.1016/j.dsr2.2017.11.009.
- He, G., Ma, W., Song, C., Yang, S., Zhu, B., Yao, H., Jiang, X., Cheng, Y., 2011. Distribution characteristics of seamount cobalt-rich ferromanganese crusts and the determination of the size of areas for exploration and exploitation. Acta Oceanol. Sin. 30, 63–75. https://doi.org/10.1007/s13131-011-0120-9.
- Heck, K.L., van Belle, G., Simberloff, D., 1975. Explicit calculation of the rarefaction diversity measurement and the determination of sufficient sample size. Ecology 56 (6), 1459–1461. https://doi.org/10.2307/1934716.
- Hein, J.R., 2002. Cobalt-rich ferromanganese crusts: Global distribution, composition, origin and research activities. In: International Seabed Authority Technical Study No. 2. International Seabed Authority, Kingston, Jamaica.
- Henson, S.A., Sanders, R., Madsen, E., 2012. Global patterns in efficiency of particulate organic carbon export and transfer to the deep ocean. Global Biogeochem. Cycles 26. https://doi.org/10.1029/2011GB004099.
- Horton, T., Marsh, L., Bett, B.J., Gates, A.R., Jones, D.O.B., Benoist, N.M.A., Pfeifer, S., Simon-Lledó, E., Durden, J.M., Vandepitte, L., Appeltans, W., 2021.
   Recommendations for the Standardisation of Open Taxonomic Nomenclature for Image-Based Identifications. Front. Mar, Sci, p. 8.
- Jiang, X., Dong, C., Ji, Y., Wang, C., Shu, Y., Liu, L., Ji, J., 2021. Influences of deep-water seamounts on the hydrodynamic environment in the northwestern Pacific Ocean. J. Geophys. Res. Oceans 126, e2021JC017396. https://doi.org/10.1029/ 2021JC017306
- Legendre, P., 2014. Interpreting the replacement and richness difference components of beta diversity. Glob. Ecol. Biogeogr. 23, 1324–1334. https://doi.org/10.1111/ cebl.13007
- Legendre, P., Anderson, M.J., 1999. Distance-based redundancy analysis: testing multispecies responses in multifactorial ecological experiments. Ecol. Monogr. 69, 1–24. https://doi.org/10.1890/0012-9615(1999)069[0001:DBRATM]2.0.CO;2.
- Legendre, P., De Cáceres, M., 2013. Beta diversity as the variance of community data: dissimilarity coefficients and partitioning. Ecol. Lett. 16, 951–963. https://doi.org/ 10.1111/ele.12141.
- Legendre, P., Legendre, L., 2012. In: Numerical Ecology, third ed. Elsevier Science BV, Amsterdam.
- Levin, L.A., Etter, R.J., Rex, M.A., Gooday, A.J., Smith, C.R., Pineda, J., Stuart, C.T., Hessler, R.R., Pawson, D., 2001. Environmental influences on regional deep-sea species diversity. Annu. Rev. Ecol. Syst. 32, 51–93. https://doi.org/10.1146/ annurev.ecolsvs.32.081501.114002.
- McClain, C.R., Lundsten, L., 2015. Assemblage structure is related to slope and depth on a deep offshore Pacific seamount chain. Mar. Ecol. 36, 210–220. https://doi.org/ 10.1111/maec.12136.
- McClain, C.R., Lundsten, L., Barry, J., DeVogelaere, A., 2010. Assemblage structure, but not diversity or density, change with depth on a Northeast Pacific seamount. Mar. Ecol. 31, 14–25. https://doi.org/10.1111/j.1439-0485.2010.00367.x.
- Meyer, D.L., 1979. Length and spacing of the tube feet in crinoids (echinodermata) and their role in suspension-feeding. Mar. Biol. 51, 361–369. https://doi.org/10.1007/
- Moraitis, M.L., Karakassis, I., 2020. Assessing large-scale macrobenthic community shifts in the Aegean Sea using novel beta diversity modelling methods. Ramifications on environmental assessment. Sci. Total Environ. 734, 139504 https://doi.org/ 10.1016/j.scitotenv.2020.139504.
- Morato, T., Pham, C.K., Pinto, C., Golding, N., Ardron, J.A., Durán Muñoz, P., Neat, F., 2018. A multi criteria assessment method for identifying vulnerable marine ecosystems in the north-East Atlantic. Front. Mar. Sci. 5, 460. https://doi.org/ 10.3389/fmars.2018.00460.

- Morgan, N.B., Cairns, S., Reiswig, H., Baco, A.R., 2015. Benthic megafaunal community structure of cobalt-rich manganese crusts on Necker ridge. Deep Sea res. Part Oceanogr. Res. Pap. 104, 92–105. https://doi.org/10.1016/j.dsr.2015.07.003.
- Morgan, N.B., Goode, S., Roark, E.B., Baco, A.R., 2019. Fine Scale Assemblage Structure of Benthic Invertebrate Megafauna on the North Pacific Seamount Mokumanamana. Front. Mar, Sci, p. 6.
- Na, J., Chen, W., Zhang, D., Zhang, R., Lu, B., Shen, C., Zhou, Y., Wang, C., 2021. Morphological description and population structure of an ophiuroid species from cobalt-rich crust seamounts in the Northwest Pacific: implications for marine protection under deep-sea mining. Acta Oceanol. Sin. 40, 79–89. https://doi.org/10.1007/s13131-020-1666-1.
- Perez, J.A.A., Kitazato, H., Sumida, P.Y.G., Sant'Ana, R., Mastella, A.M., 2018. Benthopelagic megafauna assemblages of the Rio Grande rise (SW Atlantic). Deep Sea res. Part Oceanogr. Res. Pap. 134, 1–11. https://doi.org/10.1016/j.dsr 2018 03 001
- Perez, J.A.A., Vizuete, R.S., Ramil, F., Castillo, S., 2022. Fish, cephalopods and associated habitats of the discovery rise seamounts, Southeast Atlantic. Deep Sea Res. Part Oceanogr. Res. Pap. 188, 103849 https://doi.org/10.1016/j.dsr.2022.103849.
- Preez, C.D., Curtis, J.M.R., Clarke, M.E., 2016. The structure and distribution of benthic communities on a shallow seamount (cobb seamount, Northeast Pacific Ocean). PLoS One 11, e0165513. https://doi.org/10.1371/journal.pone.0165513.
- Puerta, P., Mosquera-Giménez, Á., Reñones, O., Domínguez-Carrió, C., Rueda, J.L., Urra, J., Carreiro-Silva, M., Blasco-Ferre, J., Santana, Y., Gutiérrez-Zárate, C., Vélez-Belchí, P., Rivera, J., Morato, T., Orejas, C., 2022. Variability of deep-sea megabenthic assemblages along the western pathway of the Mediterranean outflow water. Deep Sea Res. Part Oceanogr. Res. Pap. 185, 103791 https://doi.org/10.1016/j.dsr.2022.103791.
- Rex, M.A., Etter, R.J., 2010. Deep-Sea Biodiversity: Pattern and Scale. Harvard University Press, Cambridge.
- Roberts, E.M., Bowers, D.G., Meyer, H.K., Samuelsen, A., Rapp, H.T., Cárdenas, P., 2021. Water masses constrain the distribution of deep-sea sponges in the North Atlantic Ocean and Nordic seas. Mar. Ecol. Prog. Ser. 659, 75–96. https://doi.org/10.3354/ meps13570.
- Rogacheva, A., Gebruk, A., Alt, C.H.S., 2012. Swimming deep-sea holothurians (Echinodermata: Holothuroidea) on the northern mid-Atlantic ridge. Zoosymposia 7, 213–224. https://doi.org/10.11646/zoosymposia.7.1.19.
- Rogers, A.D., 1994. The biology of seamounts. In: Blaxter, J.H.S., Southward, A.J. (Eds.), Advances in Marine Biology. Academic Press, pp. 305–350. https://doi.org/10.1016/S0065-2881(08)60065-6.
- Rogers, A.D., 2018. Chapter four the biology of seamounts: 25 years on. In: Sheppard, C. (Ed.), Advances in Marine Biology. Academic Press, pp. 137–224. https://doi.org/10.1016/bs.amb.2018.06.001.
- Rowden, A.A., Leduc, D., Clark, M.R., Bowden, D.A., 2016. Habitat differences in deep-sea megafaunal communities off New Zealand: implications for vulnerability to anthropogenic disturbance and management. Front. Mar. Sci. 3 https://doi.org/10.3389/fmars.2016.00241.
- Schlacher, T.A., Baco, A.R., Rowden, A.A., O'Hara, T.D., Clark, M.R., Kelley, C., Dower, J.F., 2014. Seamount benthos in a cobalt-rich crust region of the Central Pacific: conservation challenges for future seabed mining. Divers. Distrib. 20, 491–502. https://doi.org/10.1111/ddi.12142.
- Shen, C., Lu, B., Li, Z., Zhang, R., Chen, W., Xu, P., Yao, H., Chen, Z., Pang, J., Wang, C., Zhang, D., 2021. Community structure of benthic megafauna on a seamount with cobalt-rich ferromanganese crusts in the northwestern Pacific Ocean. Deep Sea Res. Part Oceanogr. Res. Pap. 178, 103661 https://doi.org/10.1016/j.dsr.2021.103661.
- Sommer, B., Harrison, P.L., Beger, M., Pandolfi, J.M., 2014. Trait-mediated environmental filtering drives assembly at biogeographic transition zones. Ecology 95, 1000–1009. https://doi.org/10.1890/13-1445.1.
- UNGA, 2006. Resolution 61/105. Sustainable Fisheries, Including Through the 1995 Agreement for the Implementation of the Provisions of the United Nations Convention on the Law of the Sea of 10 December1982 Relating to the Conservation and Management of Straddling Fish Stocks and Highly Migratory Fish Stocks, and Related Instruments. United Nations General Assembly. Available at. http://www.un.org/Depts/los/general\_assembly/general\_assembly\_reports.htm.
- Victorero, L., Robert, K., Robinson, L.F., Taylor, M.L., Huvenne, V.A.I., 2018. Species replacement dominates megabenthos beta diversity in a remote seamount setting. Sci. Rep. 8, 4152. https://doi.org/10.1038/s41598-018-22296-8.
- Wagner, D., Friedlander, A.M., Pyle, R.L., Brooks, C.M., Gjerde, K.M., Wilhelm, T., Aulani, 2020. Coral Reefs of the High Seas: Hidden Biodiversity Hotspots in Need of Protection. Front. Mar, Sci, p. 7.
- Wang, M., Wu, Z., Best, J., Yang, F., Li, X., Zhao, D., Zhou, J., 2021. Using multibeam backscatter strength to analyze the distribution of manganese nodules: a case study of seamounts in the Western Pacific Ocean. Appl. Acoust. 173, 107729 https://doi. org/10.1016/j.apacoust.2020.107729.
- Watling, L., Auster, P.J., 2021. Vulnerable marine ecosystems, communities, and indicator species: confusing concepts for conservation of seamounts. Front. Mar. Sci. 8, 622586 https://doi.org/10.3389/fmars.2021.622586.
- Williams, A., Schlacher, T.A., Rowden, A.A., Althaus, F., Clark, M.R., Bowden, D.A., Stewart, R., Bax, N.J., Consalvey, M., Kloser, R.J., 2010. Seamount megabenthic assemblages fail to recover from trawling impacts. Mar. Ecol. 31, 183–199. https://doi.org/10.1111/j.1439-0485.2010.00385.x.
- Wilson, R.R., Smith, K.L., Rosenblatt, R.H., 1985. Megafauna associated with bathyal seamounts in the central North Pacific Ocean. Deep Sea res. Part Oceanogr. Res. Pap. 32, 1243–1254. https://doi.org/10.1016/0198-0149(85)90007-X.

- Yesson, C., Clark, M.R., Taylor, M.L., Rogers, A.D., 2011. The global distribution of seamounts based on 30 arc seconds bathymetry data. Deep Sea res. Part Oceanogr. Res. Pap. 58, 442–453. https://doi.org/10.1016/j.dsr.2011.02.004.
  Yesson, C., Taylor, M.L., Tittensor, D.P., Davies, A.J., Guinotte, J., Baco, A., Black, J.,
- Hall-Spencer, J.M., Rogers, A.D., 2012. Global habitat suitability of cold-water
- octocorals. J. Biogeogr. 39, 1278-1292. https://doi.org/10.1111/j.1365-2699.2011.02681.x.
- Young, C.M., Tyler, P.A., Cameron, J.L., Rumrill, S.G., 1992. Seasonal breeding aggregations in low-density populations of the bathyal echinoid Stylocidaris lineata. Mar. Biol. 113, 603–612. https://doi.org/10.1007/BF00349704.